Probabilistic forecasts of temperature and precipitation change based on global climate model simulations (CES deliverable 2.2)

Jouni Räisänen[1]
Kimmo Ruosteenoja[2]

19 December 2008

[1] Department of Physics, P.O. Box 64, FI-00014 University of Helsinki, Finland
Email: jouni.raisanen@helsinki.fi

[2] Finnish Meteorological Institute, P.O. Box 503, FI-00101 Helsinki, Finland
Email: kimmo.ruosteenoja@fmi.fi

Table of Contents

Abstract

Probabilistic forecasts of temperature and precipitation change for the period preceding the year 2050 are presented, based on the results of 19 global climate models and using two alternative techniques. As the best estimate, the models indicate a warming of climate that is largest in winter and increases from the Atlantic Ocean towards the Arctic Ocean and northern Russia. This warming is quite large compared with natural interdecadal temperature variability. Thus, with the exception of the North Atlantic area, there is already during the decade 2011-2020 at least a 95% probability that the 10-year annual mean temperature will be higher than the mean value for the baseline period 1971-2000. On the other hand, there is a lot of quantitative uncertainty in the magnitude of the temperature changes, particularly in winter when natural temperature variability is largest. The models also suggest an increase in precipitation, which is generally greatest and most certain (smallest and least certain) in winter (summer). However, in comparison with natural variability, the simulated greenhouse-gas-induced precipitation changes are weaker than changes in temperature. Thus, for example, the probability that the mean annual precipitation in 2011-2020 in northern Europe will exceed the mean for 1971-2000 is only 60-80%, depending on the region considered. However, the probability increases in later decades when the signal of greenhouse-gas-induced climate change becomes stronger. The sensitivity of the findings to the evolution of greenhouse gas emissions was also studied, by comparing forecasts derived for the SRES B1, A1B and A2 scenarios. However, due to the relatively short time frame considered, this source of uncertainty proved to be smaller than the uncertainties arising from natural climate variability and differences among climate models.

We also tested one of the two techniques in hindcast mode, to inspect its capability to capture the observed temperature and precipitation changes between the periods 1961-1990 and 1991-2005. The observed temperature and particularly precipitation changes exhibited much more small-scale geographical and seasonal variability than the best-estimate changes inferred from the model simulations, evidently because the observed changes were strongly affected by natural variability. Yet, the simulated and observed warming are of the same order of magnitude and the observed temperature and precipitation changes both generally fall within the 5-95% uncertainty range inferred from the probabilistic hindcast.

1. Introduction

Despite the strong scientific consensus that increases in atmospheric greenhouse gases will lead to substantial changes in the global climate during this century (IPCC 2007), estimates of the magnitude (and for some aspects of climate, the direction) of the forthcoming changes are uncertain. This uncertainty comes from three basic sources:

- **Scenario uncertainty**: future changes in the atmospheric composition, and thus the external forcing of the climate system, depend on the magnitude of future anthropogenic emissions of greenhouse gases and other radiatively active substances such as aerosol particles and their precursor gases.
- **Modelling uncertainty** that results from our incomplete understanding, and incomplete capability to describe in climate models, the dynamics of the climate system that determine its response to changes in external forcing.
- **Natural climate variability**, resulting in part from variations in solar and volcanic activity but at least as importantly from the internal dynamics of the climate system, will continue alongside the gradual anthropogenic climate changes.

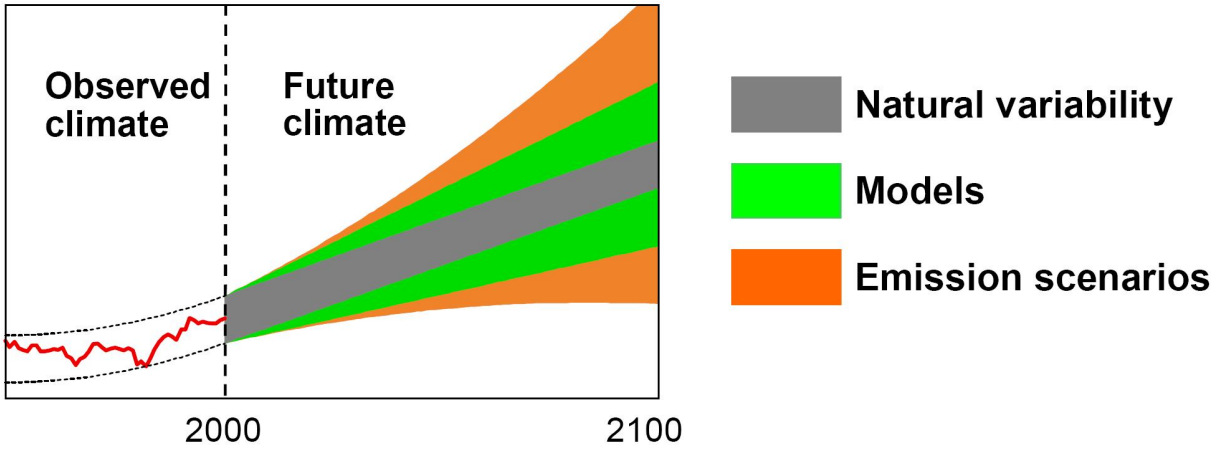

Figure 1.1. *A schematic view of sources of uncertainty in climate change as a function of time (see text for further discussion).*

The relative importance of these uncertainties depends on the time period considered (Figure 1.1). Scenario uncertainty is very important in the long run. For example, the Intergovernmental Panel on Climate Change best estimates for the global mean temperature change by the end of the 21st century vary from 1.8°C to 4.0°C between the SRES scenarios with the smallest (B1) and the largest (A1FI) greenhouse gas emissions (IPCC 2007). For shorter time horizons, however, the scenario uncertainty is much smaller. On one hand, there is inertia in the socio-economical system, and the various scenarios of greenhouse gas emissions therefore still stay relatively close to one another for the next few decades. On the

other hand, the atmospheric concentrations of carbon dioxide and other long-lived greenhouse gases react relatively slowly to the changes in emissions.

Modelling uncertainty is in the short run more important than scenario uncertainty, and it also increases with time. The larger the greenhouse gas forcing becomes, the larger absolute effect model errors will have in simulating the response to this forcing. Analogously, the modelling uncertainty is (in the long run) largest for scenarios with large greenhouse gas emissions. Thus, the IPCC (2007) uncertainty range for the 21st century global mean temperature increase for the lowest (B1) emission scenario (1.1-2.9°C) is in absolute terms much narrower than the uncertainty range for the highest (A1FI) scenario (2.4-6.4°C).

Natural variability is generally expected to be the dominating source of uncertainty in short-term climate projections. In high latitudes, in particular, climate is characterized by large interannual and interdecadal variability, which is difficult to predict in any detail even for the near-term future[1]. The uncertainty associated with natural variability does not actually decrease with time: even if there were no other uncertainties, it would still be at least as difficult, and probably more difficult, to forecast the temperatures for the end of this century than for the next decade. However, in comparison with the other, increasing uncertainties, natural variability becomes relatively less important with time.

The depiction of uncertainties in Figure 1.1 is schematic, not quantitative. In addition to the forecast time horizon, the relative importance of the three sources of uncertainty depends on the variable, season and geographical area considered. In particular, natural variability is expected to be relatively more important for local and regional than for global mean climate changes (because, in the global mean, contrasting regional effects of natural variability largely average out). On the other hand, natural variability is expected to be relatively less important for changes in temperature than for changes in many other variables including precipitation, because the greenhouse-gas-induced climate change signal is stronger for temperature than for other variables.

This report aims to present probabilistic forecasts (or "projections") of temperature and precipitation change for northern Europe under the period 2011-2050, taking into account the

[1] Some fraction of natural climate variability might be predictable via a proper initialization of the ocean circulation in climate models (e.g., Keenlyside et al. 2008), or if natural external forcing such as variations in the solar constant could be predicted in advance. However, the research on this subject is still in its infancy, and current understanding suggests that even the potentially predictable fraction of variability in Nordic land areas is modest (e.g., Boer 2000).

most important uncertainties. As implied by the preceding discussion, these main uncertainties include natural climate variability and, particularly towards the end of the period, uncertainty in climate modelling. For completeness, we also briefly consider the impact of emission scenario uncertainty, although this turns out to be (for the time range considered) relatively small.

The methods and model simulations used for deriving the forecasts are described in the following section. Readers who are primarily interested in the actual results may wish to skip at least parts of this section and jump directly to Section 3.

2. Data and methods

Our probabilistic forecasts are based on simulations performed with 19 global climate models (GCMs) participating in the Third Coupled Model Intercomparison Project, CMIP3 (Meehl et al. 2007). A few models in the full CMIP3 data base are excluded because of poor description of the land-sea geography in the Nordic area, severe problems in the simulation of present-day climate, or limited data availability; those included in the present analysis are listed in Table 2.1.

Some potential limitations of using the CMIP3 ensemble for probabilistic climate change forecasting should be mentioned. First, current GCMs still have a relatively coarse horizontal resolution. Within the CMIP3 ensemble, the grid spacing varies from 1.1° latitude × 1.1° longitude to 4° latitude × 5° longitude (for the analysis presented here, all the model results were interpolated onto a common 2.5° × 2.5° latitude-longitude grid). Thus, the models cannot describe local-scale variations in climate change, which might be significant particularly for precipitation in geographically complex areas. Second, it is not known whether the models in the ensemble are sufficiently different to fully encompass the modelling uncertainty discussed in the introduction. Finally, the CMIP3 models were driven by prescribed greenhouse gas concentrations, all using the same concentration scenarios for each emission scenario. Thus, the uncertainty associated with the conversion from emissions to greenhouse gas concentrations is ignored. Such uncertainty arises, in particular, from the impact of climate change on the carbon cycle (Friedlingstein et al. 2006), although this source of uncertainty is fortunately only expected to become important in the long run. Despite these limitations, we consider the CMIP3 ensemble to provide a reasonable basis for probabilistic forecasts of near-term climate change. This conclusion is also tentatively supported by the hindcast verification test described in Section 6 of this report.

Table 2.1 *The models used in this report.*

Model	Institution
BCCR-BCM2.0	Bjerknes Centre for Climate Research, Norway
CGCM3.1 (T47)	Canadian Centre for Climate Modelling and Analysis
CGCM3.1 (T63)	same as previous
CNRM-CM3	Météo-France
CSIRO-MK3.0	CSIRO Atmospheric Research, Australia
ECHAM5/MPI-OM	Max Planck Institute (MPI) for Meteorology, Germany
ECHO-G	University of Bonn and Model & Data Group, Germany; Korean Meteorological Agency
GFDL-CM2.0	Geophysical Fluid Dynamics Laboratory, USA
GFDL-CM2.1	same as previous
GISS-ER	Goddard Institute for Space Studies, USA
INM-CM3.0	Institute for Numerical Mathematics, Russia
IPSL-CM4	Institut Pierre Simon Laplace, France
MIROC3.2 (hires)	Center for Climate System Research, National Institute for Enviromental Studies and Frontier Research Center for Global Change, Japan
MIROC3.2 (medres)	same as previous
MRI-CGCM2.3.2	Meteorological Research Institute, Japan
NCAR-CCSM3	National Center for Atmospheric Research, USA
NCAR-PCM	same as previous
UKMO-HadCM3	Hadley Centre for Climate Prediction and Research / Met Office, UK
UKMO-HadGEM	same as previous

Two alternative methods for deriving probabilistic climate change forecasts from the CMIP3 data base are compared:

- Most of the results shown in this report are based on a so-called **resampling ensemble technique**. The resampling, which is described in detail in Räisänen and Ruokolainen (2006), attempts to maximize the sample size for plausible combinations of anthropogenic climate change and natural variability. We also use the "variance correction" introduced by Ruokolainen and Räisänen (2007). This correction assumes

that errors in simulated variability are independent of time scale. Thus, for example, a model that underestimates precipitation or temperature variability on the interannual time scale is also assumed to do this on interdecadal scales (and hence the distribution obtained from this model is inflated). The variance correction is only used over land areas where sufficient observational data are available. In practice, this correction is more important for precipitation than temperature forecasts (Ruokolainen and Räisänen 2007). Another underlying assumption in the method is that the probability distribution of climate changes depends only on the simulated multi-model mean global mean warming. This assumption is not exactly valid, but analysis of model simulation suggests that it is a very reasonable first approximation (Räisänen and Ruokolainen 2006; Giorgi 2008).

- Some results are also shown for a simpler technique in which a normal distribution is fitted directly to the climate change estimates obtained from the individual models. In particular, while the resampling ensemble technique is here only applied to simulations for the A1B emission scenario, the normal distribution technique is also used to derive probability distributions of climate change for the B1 (lower greenhouse gas emissions) and A2 (higher greenhouse gas emissions) scenarios.

In both methods, all available models are assumed to deserve the same weight in the calculations. In the resampling ensemble technique, only one simulation of climate change is used for each model. In the normal distribution method, by contrast, all simulations for the same model and emission scenario are averaged, for those models and scenarios for which more than one parallel simulation is available. This aims at reducing the effects of natural variability. As a result, the normal distribution method gives in most cases slightly narrower uncertainty intervals of climate change than the resampling method (Section 7).

In the following, we start by discussing the results obtained with the resampling ensemble method. First, in Sections 3-5, both best estimates and probabilistic forecasts of climate change for the next four decades (2011-2020 to 2041-2050) are given. Then, in Section 6, the resampling method is tested in hindcast mode, by studying how well the method is able to forecast the temperature and precipitation changes that occurred between the periods 1961-1990 and 1991-2005. In Section 7, forecasts from the resampling method and the normal distribution method are compared with each other. This section also assesses, by using the normal distribution method, the sensitivity of the forecasts to the choice between the SRES B1, A1B and A2 scenarios. Finally, the main conclusions are summarized in Section 8.

To make the report easier to read, only the most essential figures are included within the main text. A number of additional maps and diagrams are given in an appendix. In any case, it is

not feasible to show in printed form all the information available from the models. Thus, although this report shows detailed ”local” probabilistic forecasts of temperature and precipitation change for a few individual locations, these are only given as examples. Similar results can be produced for other locations if requested by the end users within the CES project.

Throughout this report, changes in climate are calculated using the mean values for 1971-2000 as the reference. Thus, for example, a 5% increase in precipitation implies 5% more precipitation than during the years 1971-2000 on the average

3. Best estimates of temperature and precipitation change

First, best estimates of near-future temperature and precipitation change are briefly discussed. These best estimates are here defined as the medians of the distributions obtained by the resampling ensemble method under the SRES A1B scenario. Thus, both smaller and larger changes are expected to have a 50% probability of occurrence.

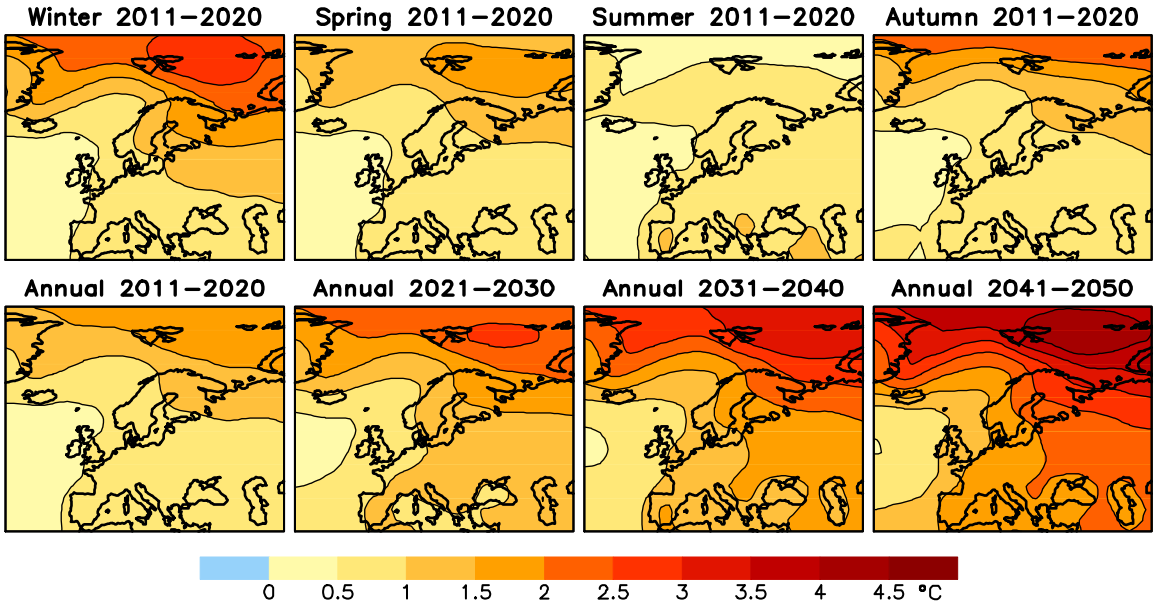

Figure 3.1. *Best estimates of temperature change. The top row represents temperature changes for the decade 2011-2020 in four three-month seasons (winter = December-January-February; spring = March-April-May; summer = June-July-August; autumn = September-October-November). The bottom row shows the best estimates of annual mean temperature change as a function of time, from 2011-2020 to 2041-2050. All changes are expressed relative to the mean temperature in 1971-2000. Shading interval is 0.5ºC, as indicated by the colour bar.*

These best-estimate changes depend on the time of the year, and they increase in magnitude when looking further into the future. This is illustrated for temperature changes in Figure 3.1, which shows that:

- The projected warming in northern Europe is largest in winter (defined here as December-January-February) and smallest in summer (June-July-August).
- The warming is generally projected to increase from southwest to northeast, from the Atlantic Ocean towards northern Russia and the Arctic Ocean. This contrast is particularly large in winter. In summer, however, the warming over the Arctic Ocean is small, and there is a maximum of warming in southern Europe.
- As the best estimate, the mean winter temperatures in the next full decade (2011-2020) are projected to exceed their mean value for 1971-2000 by 0.5-1°C in Iceland, but by up to 1.5-2°C in northeastern Finland and northwestern Russia. The corresponding best estimate for warming in summer is less than 1°C everywhere in northern Europe.
- The best-estimate warming proceeds more or less linearly in time (see the bottom row of Figure 3.1). The projected annual mean temperature increase by the decade 2041-2050 is more than twice the increase by the decade 2011-2020, varying from about 1.5°C in Iceland to 2.5-3°C in northeastern Finland and northwestern Russia.

Both the geographical pattern and the seasonal distribution of the best-estimate warming are nearly independent of time. Maps of the best-estimate temperature change for the individual three-month seasons for each of the decades 2011-2020, 2021-2030, 2031-2040 and 2041-2050 are shown in the Appendix (Figure A3.1).

A similar set of maps for best-estimate precipitation changes is shown in Figure 3.2. There is a marked contrast between increasing precipitation in northern and decreasing precipitation in southern Europe. This pattern shifts with the seasons, so that the border between increasing and decreasing precipitation is located further in the north in summer (around 55°N) than in winter (around 45°N). The greatest precipitation increases in continental northern Europe occur in winter, when the simulated warming is largest as well. Over the northern North Atlantic and Iceland, however, the increase in precipitation is relatively small and actually slightly smaller in winter and spring than in summer and autumn.

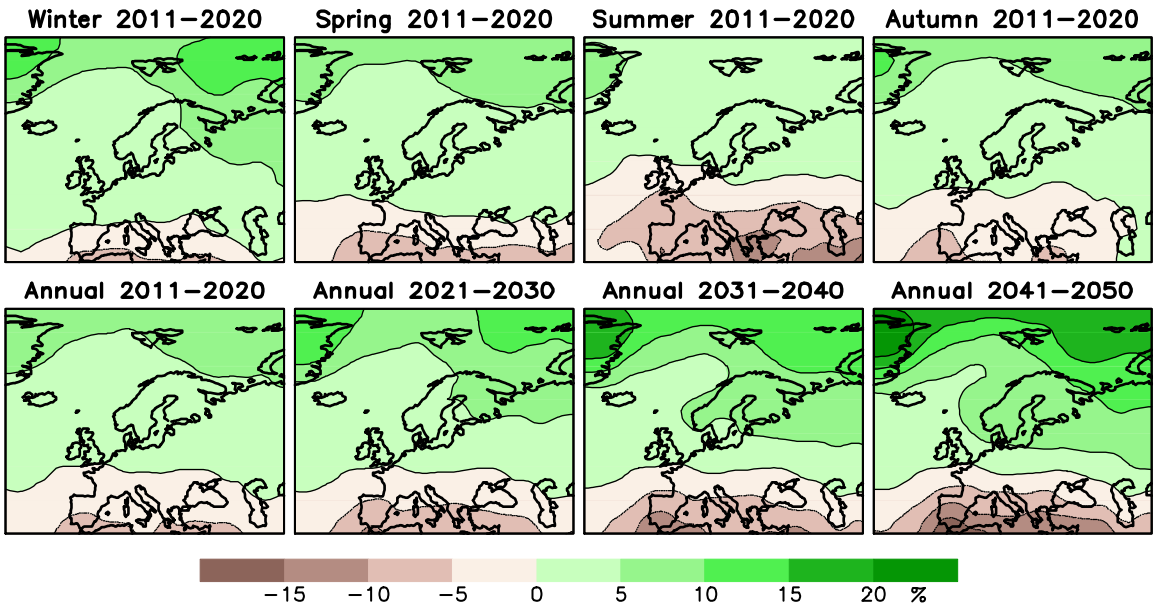

Figure 3.2. *Best estimates of precipitation change from the years 1971-2000 to the periods indicated above each panel, under the A1B emission scenario. Interval for contours and shading is 5%.*

The best-estimate precipitation changes projected for the decade 2011-2020 are still quite modest (less than 5% in northern Europe, except for slightly larger increases in the northeast in winter). Similarly to the temperature changes, however, the precipitation changes increase in magnitude with time (bottom row of Figure 3.2). For the decade 2041-2050, a best-estimate annual precipitation increase of 5-10% is projected for most of northern Europe.

As with temperature, both the geographical pattern and the seasonal distribution of the best-estimate precipitation change are nearly independent of time. Maps of the change in the individual three-month seasons for each of the decades 2011-2020, 2021-2030, 2031-2040 and 2041-2050 are shown in the Appendix (Figure A3.2).

The temperature and precipitation changes that will occur in the real world will not follow these best-estimate changes exactly. Natural climate variability may occasionally amplify, occasionally reduce or even reverse the changes that would result from the gradual increase in greenhouse gas concentrations alone. Thus, temperature and precipitation will not increase steadily from year to year or from decade to decade, although an overall trend towards warmer and wetter conditions is expected. In addition, the response of climate to increasing greenhouse gas concentrations, which determines the magnitude of these long-term trends, varies among climate models. The resulting uncertainty in the climate change projections is studied in the following two sections.

4. How certainly will temperature and precipitation increase?

As the best estimate, both temperature and precipitation will increase in the Nordic area. How certainly will the changes in the real world be of this sign?

To answer this question for the mean temperatures in the next full decade, the top row in Figure 4.1 shows, for each four seasons, the probability that the decadal mean temperature in that season will be higher in 2011-2020 than it was in 1971-2000. Over the northern parts of the European continent, a warming of climate appears very likely already in 2011-2020. The seasonal probabilities of warming vary from slightly below 90% to about 95%, depending on season and location. The corresponding probability of warming for the annual mean temperature in 2011-2020 is even higher, at least 95% (first panel in the bottom row of Figure 4.1)[2]. Note that there is little difference between the probability of warming in winter and summer: although the best-estimate warming is larger in winter than in summer, so is also the uncertainty associated with natural variability and differences between climate models.

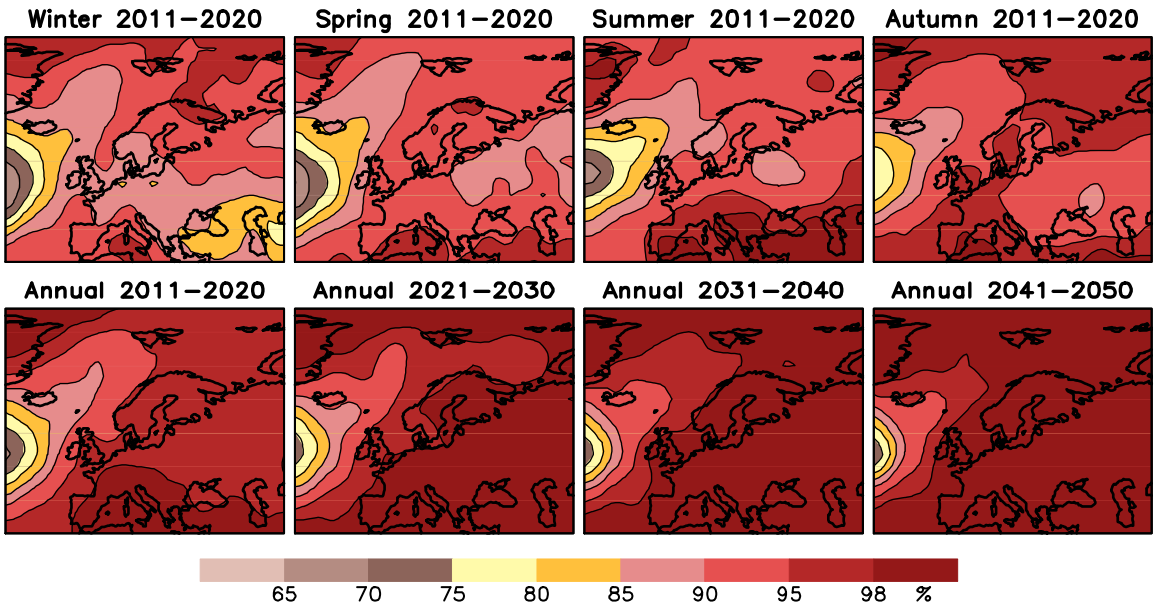

Figure 4.1. *Probability of warming, as estimated with the resampling ensemble method. The top row shows the probability that the average winter, spring, summer and autumn temperatures in the decade 2011-2020 will exceed their mean value in 1971-2000. The bottom row gives the probability of annual mean warming as a function of time, from 2011-2020 to 2041-2050. The colour scale is given below the figure.*

[2] Note that these numbers refer to the probability that the whole decade, on the average, will be warmer than the mean value for 1971-2000. The probability that the annual or seasonal mean temperature in any single year will exceed the mean for 1971-2000 is significantly lower.

Later, when the signal of greenhouse-gas-induced climate change gorws stronger, the probability of warming in Europe becomes even larger, approaching 100% for the annual mean in the decade 2041-2050 (bottom row of Figure 3.1). However, in contrast to the very high probability of warming over European land areas, the analysis suggests a substantial (up to about 30%) chance of cooling over the North Atlantic Ocean to the south of Iceland; this feature persists throughout the period studied. A 2-15% chance of cooling (depending on the time period and season considered) is found over Iceland itself. The lower probability of warming in the North Atlantic area may partly reflect the large long-term natural variability there, caused by slow variations in the North Atlantic ocean circulation. More importantly, almost all climate models simulate a decrease in the North Atlantic thermohaline circulation during the 21st century (IPCC 2007, Section 10.3.4). In some models, the associated decrease in northward heat transport is large enough to reverse the greenhouse-gas-induced warming to local cooling over parts of the North Atlantic Ocean. However, despite this decrease in the thermohaline circulation, none of the models considered in this study simulates a cooling of climate over the European continent.

Maps showing the probability of warming in the four individual seasons in all of the decades 2011-2020, 2021-2030, 2031-2040 and 2041-2050 are given in the Appendix (Figure A4.1).

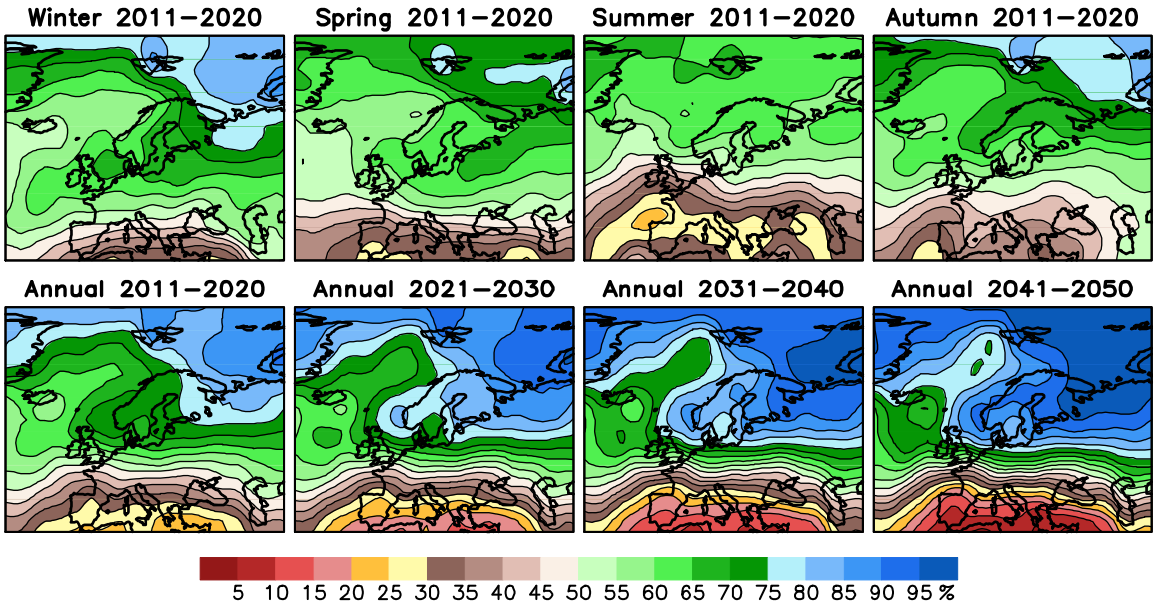

Figure 4.2. *Probability of precipitation increase, as estimated with the resampling ensemble method. The top row shows the probability that the average winter, spring, summer and autumn precipitation sums in the decade 2011-2020 will exceed their mean values in 1971-2000. The bottom row gives the probability of increasing annual mean precipitation as a function of time, from 2011-2020 to 2041-2050. The colour scale is given below the figure.*

In comparison with temperature, the sign of precipitation changes is more uncertain, particularly in the short run (Figure 4.2). For the decade 2011-2020, the probability of increasing annual mean precipitation is about 65-80% in continental northern Europe, being largest in northwestern Russia and decreasing to the south and west. In Iceland, the probability of precipitation increase on this time scale is only 60-65%. Analogously with temperature, the sign of seasonal mean precipitation changes is less certain than that of the annual mean change. Nevertheless, the probability of increasing precipitation is (with the exception of Iceland and the Atlantic Ocean) larger in winter than in summer.

As time proceeds, the signal of greenhouse-gas-induced precipitation changes becomes better discerned from natural variability. In the decade 2041-2050, the probability of increasing annual mean precipitation over Finland, north-western Russia and much of Scandinavia is 85-95%. However, even at this time, the increase in precipitation is less certain in summer than in the other seasons (Figure A4.2 in the Appendix). Another noteworthy feature is the high and gradually increasing probability of decreasing annual mean precipitation in the Mediterranean area.

Maps showing the probability of precipitation increase in the individual seasons in all of the decades 2011-2020, 2021-2030, 2031-2040 and 2041-2050 are given in the Appendix (Figure A4.2).

5. Uncertainty ranges and quantiles of temperature and precipitation change

To characterize the uncertainty range in annual mean temperature change, the 5th and 95th percentiles[3] of the calculated probability distribution are shown in Figure 5.1, decade by decade from 2011-2020 to 2041-2050. As far as the method of estimating the probabilities is valid, there is by definition a 90% probability that the changes in the real world will fall between these lower and upper estimates.

The 5th percentile of temperature change is still close to zero in the decade 2011-2020, being slightly negative over the Atlantic Ocean and slightly positive elsewhere (this is, of course, consistent with the lower-left panel of Figure 4.1, which shows a probability of annual mean warming varying on both sides of 95% at this time). As time progresses, this lower limit of the uncertainty range increases, although relatively slowly. It first exceeds 1°C in the decade 2041-2050 in Finland and northwestern Russia.

[3] The terms percentile and quantile are used here interchangeably.

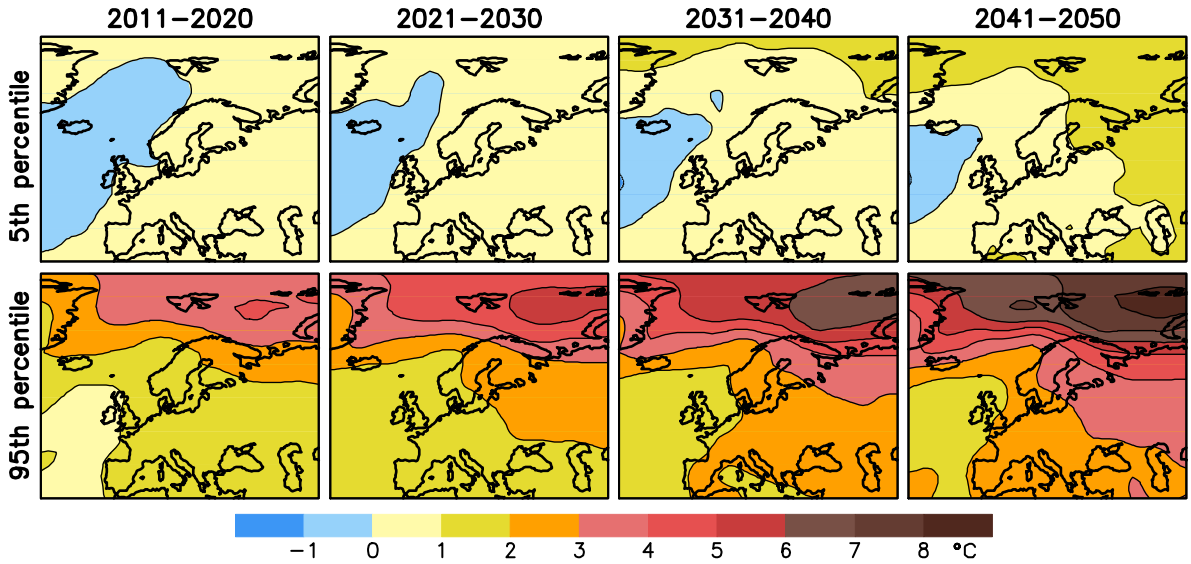

Figure 5.1. *The 5th and 95th percentiles of annual mean temperature change as a function of time, as estimated with the resampling ensemble method. There is, on the basis of the present model simulations, a 90% probability that the temperature changes in the real world will fall between the 5th and the 95th percentiles. The changes are expressed as differences from the mean temperature during 1971-2000. The colour scale is given below the figure.*

The 95th percentile of annual mean temperature change exceeds 2°C in the northern parts of the Nordic area already in the decade 2011-2020 (bottom row of Figure 4.1). Furthermore, the 95th percentile increases faster in time than the 5th percentile. Thus, the magnitude of uncertainty increases. Initially, the uncertainty is dominated by natural variability. However, when the greenhouse gas forcing becomes stronger, modelling uncertainty also increases, making the total uncertainty range wider (as suggested by the schematic presentation in Figure 1.1). In fact, the total uncertainty for the last decades is also to some extent affected by uncertainty in greenhouse gas emissions (Section 7); this source of uncertainty is not included in the analysis presented in this section.

Similar maps for the 5th and 95th percentiles of annual mean precipitation change are shown in Figure 5.2. In contrast to temperature, the 5th percentile of precipitation change remains mostly negative throughout the period studied here – thus, even in the decade 2041-2050 the probability that the mean precipitation will be lower than it was in 1971-2000 exceeds 5%. The 95th percentile typically falls between 10-15% in 2011-2020, increasing to 15-20% by 2041-2050 (except for higher values in the Arctic in both periods). Thus, precipitation changes have a rather wide uncertainty range.

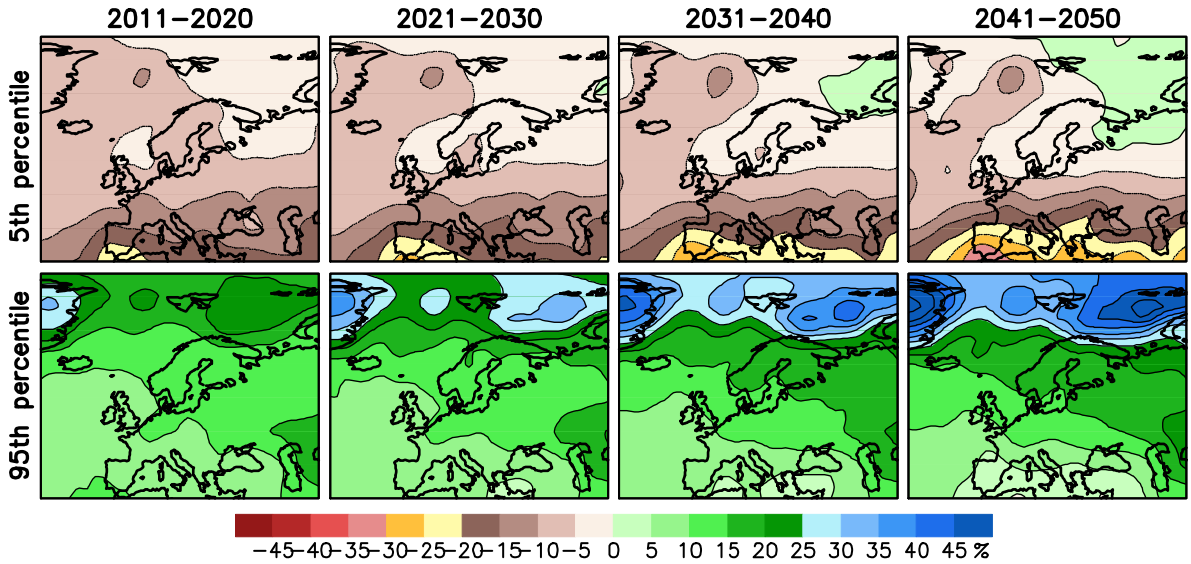

Figure 5.2. *The 5th and 95th percentiles of annual mean precipitation change as a function of time, as estimated with the resampling ensemble method. The changes are expressed as per cent differences from the mean precipitation during 1971-2000. The colour scale is given below the figure.*

Figure 5.3 provides a more detailed quantile analysis of annual mean temperature and precipitation changes for three grid boxes: the first in Iceland (65ºN, 20ºW), the second in western Norway (62.5ºN, 7.5ºW) and the third in northern Finland (67.5ºN, 27.5ºE). This selection of grid boxes is fairly arbitrary – similar plots can be produced for other locations if desired by the end users within the CES project.

As a general word of caution associated with such a local analysis, it should be stressed that these results are based on output from relatively coarse-resolution global climate models. These models are not skilful in simulating such small-scale features in climate change that might be associated with the details of the regional land-sea distribution and orography (the effects of which are expected to be captured better by regional climate models that will be used in other parts of the CES project). Nevertheless, the quantile plots for the three locations serve to exemplify the variation of the projected climate changes and their uncertainty within the Nordic area.

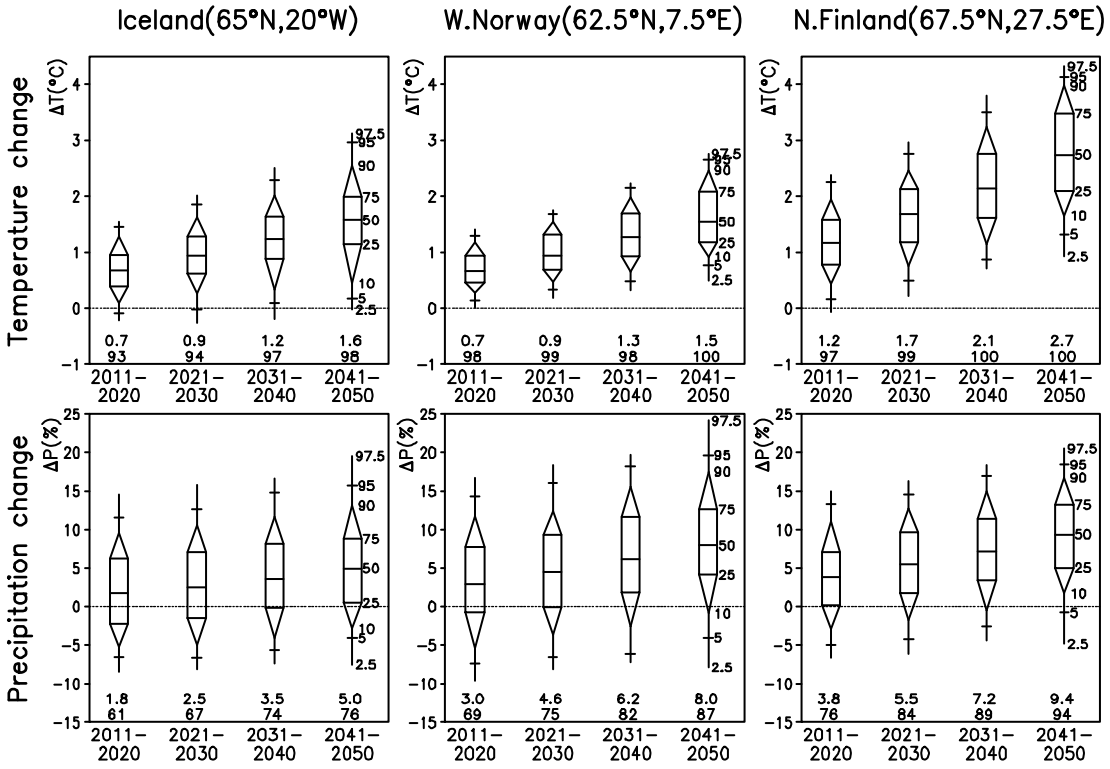

Figure 5.3. *Probabilistic forecasts of annual mean temperature (top) and precipitation (bottom) change for the three locations indicated on the top of the figure. The diagrams show the 2.5%, 5%, 10%, 25%, 50%, 75%, 90%, 95% and 97.5% quantiles of the probability distributions, separately for the four decades 2011-2020, 2021-2030, 2031-2040 and 2041-2050. The two numbers on the bottom of each panel give the median estimate of the change relative to the baseline 1971-2000 (in ºC for temperature and in per cent for precipitation), and the probability (in per cent) that the forecast period will be warmer/wetter than 1971-2000.*

In terms of temperature change (top row of Figure 5.3), the grid boxes in Iceland and western Norway are characterized by relatively slow warming in most model simulations, evidently because both are affected by the vicinity of the slowly warming Atlantic Ocean. The grid box in western Norway also has a relatively narrow uncertainty range in the temperature change. The warming in northern Finland is projected to be faster, particularly in winter, but its magnitude is associated with a rather large uncertainty. This reflects both the increase in natural temperature variability further away from the Atlantic coastline but also large scatter among the responses of different climate models to increasing greenhouse gas forcing. The figure also shows a relatively wide uncertainty range for the temperature change in Iceland, particularly for the decades 2031-2040 and 2041-2050. On the one hand, there are some models in which the decrease in the Atlantic thermohaline circulation largely negates greenhouse-gas-induced warming in Iceland. On the other hand, the warming in Iceland is quite large in a few individual models, but this feature may be unphysical. In the models with the largest warming, sea ice extends too far south in the simulated present-day climate; when

the increasing greenhouse gas forcing warms the climate, the retreat of this excessive ice cover leads to a spurious amplification of the warming, especially in winter. Thus, the upper end of the uncertainty range for the warming in Iceland may be too high, particularly for the decades 2031-2040 and 2041-2050.

As already noted, precipitation changes are more uncertain than temperature changes, mainly because the signal-to-noise ratio between the greenhouse-gas-induced changes and natural variability is lower for precipitation. Consequently there is, in all three locations included in Figure 5.3, a substantial probability that some of the next few decades might still have less precipitation than the baseline period 1971-2000. The uncertainty range in precipitation change is particularly large in western Norway. This is likely so because the amount of precipitation on the western side of the Scandinavian mountains is very sensitive to the atmospheric circulation. Thus, natural interdecadal variability in the atmospheric circulation, together with the uncertainty in the response of the circulation to increased greenhouse gas concentrations, results in a large uncertainty in precipitation change in this area.

Additional figures on the probability distributions of temperature and precipitation change are shown in the Appendix. First, a more comprehensive set of quantile maps of temperature change (Figures A5.1-A5.5) and precipitation change (Figures A5.6-A5.10) are given. These maps include the 25^{th}, 50^{th} and 75^{th}, as well as the 5^{th} and 95^{th} percentiles of change, and the four three-month seasons in addition to the annual mean. Second, Figures A5.11-A5.12 repeat the box-whisker plot presentation of Figure 5.3 for seasonal mean temperature and precipitation changes in the same three grid boxes. Two general points about that detailed analysis are worth noting:

- The uncertainty in seasonal mean climate changes is almost invariably larger than that in the annual mean change. Because the sample size is smaller for the seasonal (30 months per decade) than for the annual means (120 months per decade), the changes in seasonal mean climate are more strongly affected by natural variability than changes in the annual mean climate. Putting this the other way round, the effects of natural variability may vary in sign between the seasons (e.g., natural variability might enhance the warming in winter but reduce it in summer) and therefore tend to be partly averaged out in the annual mean.
- The uncertainty range of temperature changes is wider in winter than in the other seasons. This is mainly because natural temperature variability in northern Europe is largest in winter.

6. Hindcast verification of the resampling ensemble technique

A rigorous verification of our climate change forecasts will only be possible after the end of the forecast period – that is, a long time after the end of the CES project. However, it is still possible to study how well the proposed forecast method would have performed in forecasting climate changes that have been already observed. Thus, in this section, we use the resampling ensemble technique for forecasting (or, more literally, hindcasting) the climate changes that occurred between the periods 1961-1990 and 1991-2005. The temperature and precipitation observations used in this verification exercise are primarily adopted from the University of East Anglia Climate Research Unit (CRU) TS 2.0 data set (Mitchell et al. 2004). However, this data set only extends to the year 2002. The temperature and precipitation values for the years 2003-2005 have been estimated with the aid of the National Center for Environmental Prediction – National Center for Atmospheric Research (NCEP-NCAR) reanalysis of temperature (Kistler et al. 2001) and the GPCP (Global Precipitation Climatology Project) Version 2 (Adler et al. 2003) analysis of precipitation. The blending of these data sets with the CRU analysis is described in Räisänen (2007).

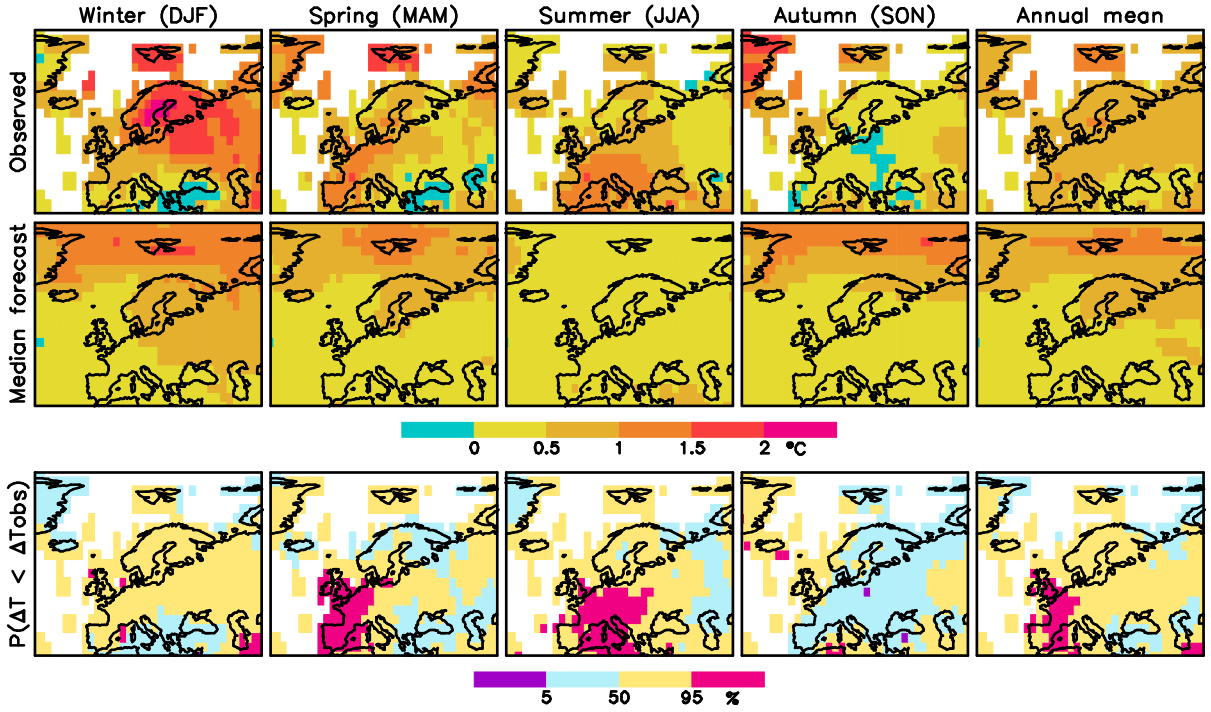

Figure 6.1. *Comparison between observed and hindcasted temperature changes from the period 1961-1990 to the period 1991-2005. First row: observed changes. Second row: best-estimate (median) changes from the model-based hindcast. Bottom row: the location of the observed change within the hindcast probability distribution. Dark red (violet) shading indicates areas where the observed change was above the 95th percentile (below the 5th percentile) of the hindcast distribution.*

The first two rows in Figure 6.1 compare the observed temperature changes with the best (median) estimate from the resampling ensemble technique. Although the observations and the hindcast broadly agree on the magnitude of the annual mean warming and they both exhibit a maximum of warming in winter, there is less agreement in the seasonal and geographical details of the change. Overall, there is much more spatial variability in the observed changes than in the best-estimate hindcast. This is not surprising, since the observations represent just one realization of climate change, which was most likely strongly affected by natural variability. By contrast, the best-estimate hindcast has been made with a method which very effectively suppresses the effects of natural variability, thus giving a relatively "clean" estimate of the forced, mostly greenhouse-gas-induced, climate change in the model simulations. Therefore, the differences between the two fields do not actually prove the hindcast method incorrect.

A more relevant question for verification of probabilistic forecasts or hindcasts is whether the observed changes fall within the forecasted probability distribution. This is addressed in the last row of Figure 6.1. The pale yellow colour indicates areas where the observed warming exceeded the median from the hindcast but still remained below its 95th percentile, whereas pale blue marks changes that fell between the 5th percentile and the median of the hindcast distribution. Only the areas shown in dark red (observed warming above the 95th percentile of the hindcast) and violet (observed change below the 5th percentile of the hindcast) are of some concern. However, even if the hindcast methodology were perfectly correct, the observed changes would still be expected to fall outside the 5-95% range on the average in 10% of the domain. Furthermore, in a relatively small area such as that depicted in Figure 5.1, this fraction may vary considerably by chance.

The actual area fraction of grid boxes in which the observed temperature changes fall outside the hindcasted 5-95% range is 11% for the annual mean change, and in the individual seasons the fraction varies between 2% (autumn) and 20% (summer). This suggests that, for the period 1991-2005, the observed temperature changes were more or less as consistent with the hindcast as statistically expected. However, with the exception of autumn, the observed temperature change falls in most areas in the upper half of the hindcast distribution, and there are much more observations above the 95th percentile than below the 5th percentile. There are at least two possible interpretations. First, it is possible that the models may have a tendency to underestimate greenhouse-gas-induced temperature changes in Europe. Another, perhaps more likely explanation is that the observed warming may have been partly natural, rather than being entirely caused by the increasing anthropogenic forcing.

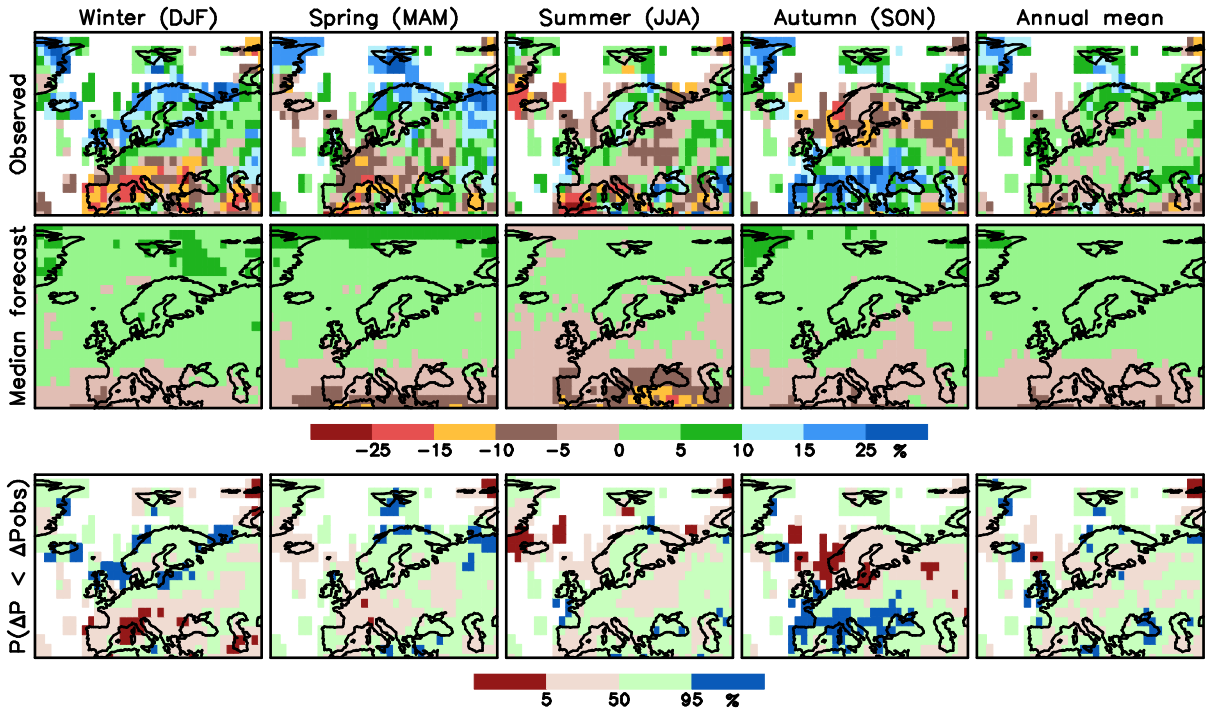

Figure 6.2. *Comparison between observed and hindcasted precipitation changes from the period 1961-1990 to the period 1991-2005. First row: observed changes. Second row: best-estimate (median) changes from the model-based hindcast. Bottom row: the location of the observed change within the hindcast probability distribution. Blue (red) shading indicates areas where the observed change was above the 95th percentile (below the 5th percentile) of the hindcast distribution.*

Figure 6.2 shows a similar analysis for precipitation change. Even when averaged over the whole year, the observed precipitation changes were geographically highly variable, although they agree with the best-estimate hindcast by being predominantly positive in northern and negative in southern Europe. The observed changes in the four individual seasons show even more irregular patterns. For example, in most of the Nordic area, winter precipitation increased substantially more than suggested by the best-estimate hindcast, whereas autumn precipitation decreased in contrast to the slight increase suggested by the models. Nevertheless, the comparison gives no obvious evidence that the hindcast method would be incorrect. The observed annual mean precipitation change was outside the 5-95% range derived from the models in only 8% of the verification domain. In the individual seasons, this fraction varies from 6% for spring and summer to 21% for autumn.

This verification analysis bears an important message for end users of climate change forecasts. It is extremely unlikely that a deterministic forecast of future climate change, regardless of how this forecast is produced, would be exactly correct. It is therefore necessary to take into account the uncertainty of the forecast rather than just rely on the most likely outcome.

7. Sensitivity to the forecast method and the emission scenario

The analysis presented this far has been based on one method of deriving the probabilities (the resampling ensemble technique) and only one emission scenario (SRES A1B) has been considered. In this section we first study the sensitivity of our results to the choice of the method, by comparing the results from the resampling ensemble technique with the more straightforward normal distribution technique mentioned in Section 2. Then, we briefly discuss the uncertainty associated with the choice of the emission scenario, by comparing the climate change projections for the A1B, B1 (lower greenhouse gas emissions) and A2 (higher greenhouse gas emissions) scenarios.

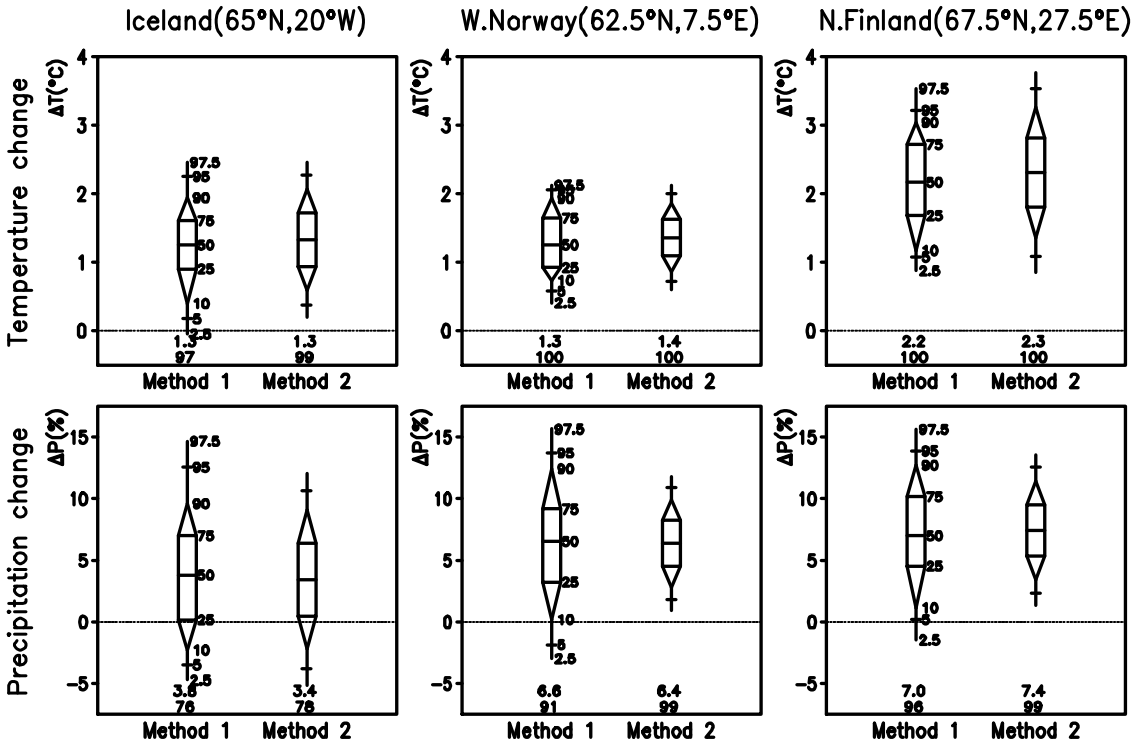

Figure 7.1. *Probability distributions of annual mean temperature (top) and precipitation (bottom) change from 1971-2000 to 2020-2049 under the SRES A1B emission scenario, at the three locations indicated on the top of the figure. Method 1 = resampling ensemble method; Method 2 = normal distribution method. The percentiles of the probability distributions are indicated in the same way as in Figure 5.3.*

In terms of the best-estimate (median) change, the resampling ensemble technique and the normal distribution method generally give very similar results. This is illustrated in Figure 7.1 for the annual mean temperature and precipitation changes at the three locations studied in Section 5.3. In this figure, the averaging period is longer than in the earlier sections (30-year

mean climate changes from 1971-2000 to 2020-2049 are considered), but virtually the same best-estimate changes would be obtained by using 2031-2040 as the forecast period.

On the other hand, the probability distributions derived using the resampling ensemble method are in most cases wider than those produced with the normal distribution method, particularly so for precipitation change. This difference stems from the different treatment of natural variability:

- In the normal distribution method, all simulations available for the same emission scenario are averaged, if more than one parallel simulation is available for a given model. As a result, the effects of natural climate variability are partly averaged out.
- In the resampling ensemble method, by contrast, an effort is made to fully represent the uncertainty that results from the combined effects of model differences and natural variability. In addition, the method attempts to correct the amplitude of simulated variability where this differs from the amplitude of observed variability. While this has relatively little effect on the forecasts of temperature change, it tends to widen the forecasted distributions of precipitation change in most locations (Ruokolainen and Räisänen 2007).

Thus, the normal distribution method gives a better approximation of the uncertainty that results directly from differences among climate models. However, when forecasting real-world climate changes, which always represent a combination of natural variability and the response to anthropogenic forcing, the uncertainty estimates from the resampling ensemble method are expected to be more realistic.

The magnitude of future climate change depends on future changes in the atmospheric composition, and hence the magnitude of anthropogenic greenhouse gas (and to some extent, aerosol) emissions. However, when the next few decades are considered, this source of uncertainty still appears to be much smaller than the uncertainties resulting from natural variability and differences among climate models.

As illustrated in Figure 7.2a for the most important anthropogenic greenhouse gas, carbon dioxide, alternative estimates of the emissions at the end of this century span a vast uncertainty range. The differences among these so-called SRES scenarios stem from different assumptions about socio-economical factors such as the growth of population and economy, technological development, and efficiency of international co-operation (Nakićenović and Swart 2000). During the next few decades, however, the range of CO_2 emissions among the same six scenarios is much narrower – all scenarios point to an increase in the emissions in

the near future, basically as a result of increasing global energy demand. Furthermore, the atmospheric CO_2 concentration reacts relatively slowly to the changes in the emissions (Figure 8.2b). Thus, for example, the range of CO_2 concentrations among the six SRES scenarios is only about 50 ppmv (parts per million in volume) in the year 2040, increasing to more than 400 ppmv by the end of the century.

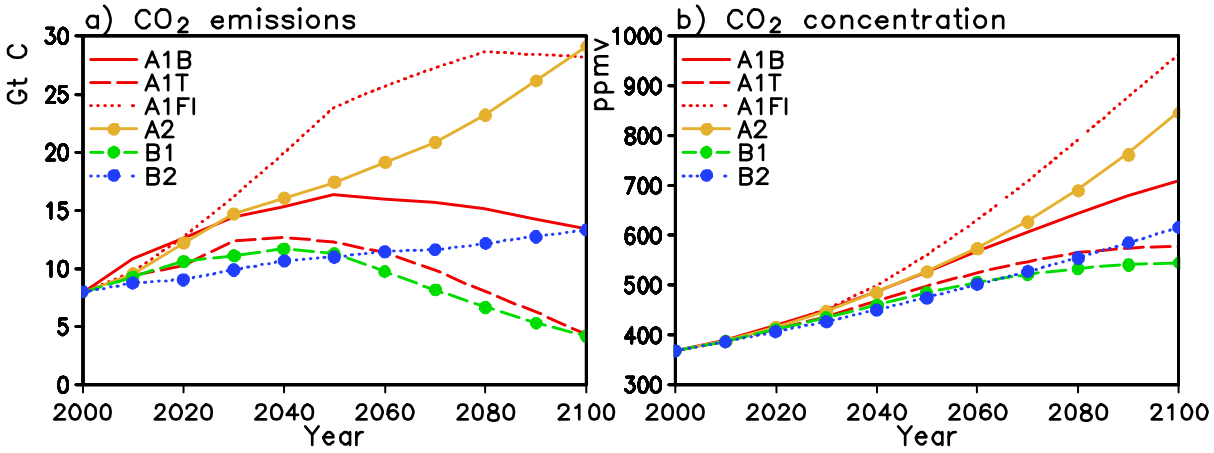

Figure 7.2. *(a) CO_2 emissions (Gt C per year) and (b) the resulting best-estimate CO_2 concentrations under six SRES emission scenarios (IPCC 2001).*

Based on the availability of climate model simulations, we selected three SRES scenarios for a closer inspection – in increasing order of emissions these are B1, A1B and A2. As can be seen from Figure 7.2, these scenarios span a considerable part of, although not the total range covered by the full set of six scenarios.

The evolution of climate change under the selected three scenarios is illustrated in Figure 7.3. For each scenario, the figure shows the best (multi-model mean) estimates of temperature and precipitation change for two areas: Finland (where the simulated changes are relatively large) and Iceland (where the changes are smaller than elsewhere in the Nordic countries). In this figure, running 9-year means are used to reduce interannual variability, and temperature and precipitation are in both cases averaged over the entire country. Despite the averaging over the 19 models and the use of the 9-year running means, the time series exhibit some irregular variability, as a residual effect of much larger natural variability in the individual model simulations. However, as expected from the corresponding differences in the concentrations of CO_2 and other greenhouse gases, the temperature and precipitation changes at the end of this century are 50-75% larger for the high-emission A2 than for the low-emission B1 scenario. A1B falls between these two cases, although it remains quite close to A2 until about the year 2080.

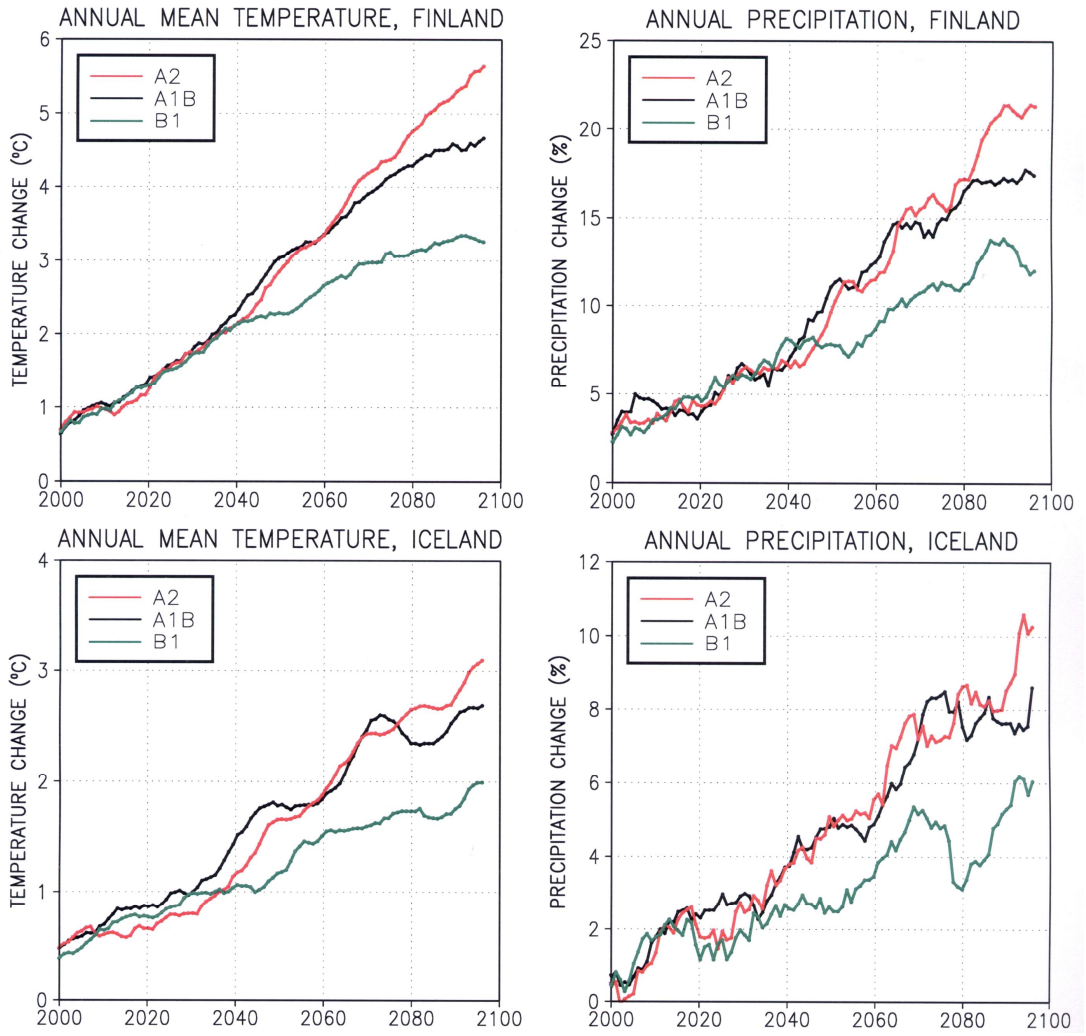

Figure 7.3. *Multi-model mean changes in annual mean temperature (left) and precipitation (right) in Finland (top) and Iceland (bottom) under the SRES B1 (green), A1B (black) and A2 (red) scenarios. The changes are expressed as differences from the means of the baseline period 1971-2000. A 9-year running mean has been used for smoothing the curves.*

In contrast to the situation at the end of the century, the differences among the three scenarios in the early 21st century are small. The multi-model mean temperature and precipitation changes in Finland remain virtually independent of the scenario until the year 2040. In Iceland, slightly larger differences occur, although this impression is amplified by the fact that the vertical scales in Figure 7.3 differ between the two countries. Even in Iceland, however, the differences between the scenarios remain negligible up to the year 2030.

Figure 5.3 showed that, in individual locations of Iceland and Finland, the 5-95% range of annual mean temperature change for the decade 2041-2050 has a width of over 2.5ºC under the A1B scenario, whereas the corresponding uncertainty range for the annual mean precipitation change is about 20%. For the same decade, the differences in multi-model mean temperature change between the B1, A1B and A2 scenarios are of the order of 0.5ºC, while

the corresponding differences in precipitation change are only about 2 percentage units (Figure 7.3). Although these three scenarios do not span the full range of emission scenario uncertainty, it can be concluded that, when approaching the middle of this century, inter-scenario differences are still small compared with the other uncertainties in climate change. This justifies our focus on only one (A1B) scenario when deriving the probabilistic forecasts represented in Sections 3-5 of this report.

8. Conclusions

In this report, we have studied the characteristics and uncertainties of temperature and precipitation change projections in northern Europe during the first half of the 21st century, using simulations performed with nearly twenty global climate models. Our main findings are:

- The ongoing increase in atmospheric greenhouse gas concentrations is expected to lead to widespread warming and an increase in precipitation in the Nordic area (Section 3).
- The magnitude of the climate changes increases with time, with increasing greenhouse gas forcing. The changes vary with season and geographically within the Nordic area (Section 3).
- Largest increases in temperature and (in most of the Nordic area) precipitation are likely to occur in winter. Changes in summer are projected to be smaller, but increases in temperature and precipitation are also expected in this season (Section 3).
- With the exception of summer, the magnitude of warming is expected to increase from southwest to northeast, from the Atlantic Ocean towards the Arctic Ocean and northern Russia (Section 3).
- Model-simulated precipitation changes show a marked contrast between an increase in northern and a decrease in southern Europe. However, most models suggest that the borderline between increasing and decreasing precipitation is located to the south of the Nordic area even in summer when it is furthest north (Section 3).
- Exact forecasts of future climate change are impossible, due to uncertainties associated with natural variability, differences among climate models and the future evolution of greenhouse gas concentrations (Sections 1, 4, 5 and 7).
- The greenhouse-induced warming is expected to be quite large compared with natural interdecadal temperature variability. In most of the Nordic area, there is therefore at least a 95% probability that the annual mean temperature in the decade 2011-2020 will be warmer than the mean value for 1971-2000. Later, the probability of warming becomes even larger (Section 4).

- Due to the uncertainty associated with the weakening of the North Atlantic thermohaline circulation, there is a somewhat larger possibility of slight cooling in Iceland than elsewhere in the Nordic countries (Sections 4-5).
- Greenhouse-gas-induced changes in precipitation will be smaller in comparison with natural variability than changes in temperature. As a result, the probability that the mean annual precipitation in 2011-2020 will exceed the mean for 1971-2000 is only 60-80%, depending on the region considered. However, the probability increases later when the greenhouse-gas-induced climate change signal becomes stronger (Section 4).
- Even in the case of temperature, there is a lot of uncertainty in the magnitude of future change. The uncertainty ranges become wider over time, as modelling uncertainty becomes gradually more important (Section 5).
- Seasonal mean changes in climate are associated with larger uncertainty than changes in annual mean temperature and precipitation. Moreover, changes in winter temperature have a wider uncertainty range than changes in the other seasons (Section 5).
- In the long run, the magnitude of climate changes will depend substantially on the magnitude of greenhouse gas emissions, in the sense that larger emissions will lead to larger changes in climate. For the period prior to the year 2050, however, emission scenario uncertainty is much smaller than the uncertainties associated with natural variability and differences among climate models (Sections 1, 4, 5 and 7).
- The climatic change that occurred in Europe between 1961-1990 and 1991-2005 was generally consistent with the probability distributions derived using our main method. While there was no detailed agreement between the best-estimate modelled changes and the observations, the observed temperature and precipitation changes only fell in the extreme tails of the derived probability distributions approximately as often as could be expected from pure chance (Section 6).

To conclude, while it is impossible to give exact forecasts of future climate, it still seems to be possible to give reasonable estimates of the probability distributions within which climate changes in the near future will fall. To the extent that the use of such probabilistic information is technically feasible for the end-users, this is expected to be a better basis of climate-related decision-making than reliance on deterministic forecasts alone, regardless of if these deterministic forecasts are based on averaging over an ensemble of climate model simulations or on the results of a single global or regional climate model (e.g., Räisänen and Palmer 2001).

Acknowledgments

We acknowledge the international modeling groups for providing their data for analysis, the Program for Climate Model Diagnosis and Intercomparison (PCMDI) for collecting and archiving the model data, the JSC/CLIVAR Working Group on Coupled Modelling (WGCM) and their Coupled Model Intercomparison Project (CMIP) and Climate Simulation Panel for organizing the model data analysis activity, and the IPCC WG1 TSU for technical support. The IPCC Data Archive at Lawrence Livermore National Laboratory is supported by the Office of Science, U.S. Department of Energy.

References

Adler, R.F. and co-authors 2003: The Version 2 Global Precipitation Climatology Project (GPCP) Monthly Precipitation Analysis (1979-Present). *Journal of Hydrometeorology*, **4**, 1147-1167.

Boer, G.J. 2000: A study of atmosphere-ocean predictability on long time scales. *Climate Dynamics*, **16**, 469-472.

Friedlingstein, P. and co-authors 2006: Climate-carbon cycle feedback analysis: results from the C^4MIP model intercomparison. *Journal of Climate*, **19**, 3337-3353.

Giorgi, F. 2008: A simple equation for regional climate change and associated uncertainty. *Journal of Climate*, **21**, 1589-1604.

IPCC (Intergovernmental Panel on Climate Change) 2001: *Climate Change 2001: the Scientific Basis.* Cambridge University Press, 881 pp.

IPCC (Intergovernmental Panel on Climate Change) 2007: *Climate Change 2007: the Physical Science Basis*. Cambridge University Press, 996 pp.

Keenlyside, N.S, M. Latif, J. Jungclaus, L. Kornblueh and E. Roeckner 2008: Advancing decadal-scale climate prediction in the North Atlantic sector. *Nature*, **453**, 84-87.

Kistler, R. and co-authors 2001: The NCEP-NCAR 50-Year Reanalysis: Monthly Means CD-ROM and Documentation. *Bulletin of the American Meteorological Society*, **82**, 247-268.

Meehl, G.A., C. Covey, T. Delworth, M. Latif, B. McAvaney, J.F.B. Mitchell, R.J. Stouffer and K.E. Taylor 2007: The WCRP CMIP3 Multimodel Dataset: A New Era in Climate Change Research. *Bulletin of the Americal Meteorological Society*, **88**, 1383-1394.

Mitchell, T.D., T.R. Carter, P.D. Jones, M. Hulme and M. New 2004: A comprehensive set of high-resolution grids of monthly climate for Europe and the globe: the observed record (1901-2000) and 16 scenarios (2001-2100).Tyndall Centre Working Paper 55, 30 pp.

Nakićenović, N. and R. Swart (Eds.) 2000: *Emission Scenarios. A Special Report of Working Group III of the Intergovernmental Panel on Climate Change*. Cambridge University Press, 599 pp.

Räisänen, J., 2007: How reliable are climate models? *Tellus*, **59A**, 2-29.

Räisänen, J. and T. N. Palmer 2001: A probability and decision-model analysis of a multi-model ensemble of climate change simulations. *Journal of Climate*, **14**, 3212-322

Räisänen, J. and L. Ruokolainen 2006: Probabilistic forecasts of near-term climate change based on a resampling ensemble technique. *Tellus*, **58A**, 461-472.

Ruokolainen, L. and J. Räisänen 2007: Probabilistic forecasts of near-term climate change: sensitivity to adjustment of simulated variability and choice of baseline period. *Tellus*, **59A**, 309-320.

Appendix: Additional figures

The figures in this appendix are numbered following the main sections in the report. A brief list of the figures is provided below. More detailed captions are given under each figure.

Figure 3.A1. Best estimates of temperature change, as a function of decade and season.
Figure 3.A2. Best estimates of precipitation change, as a function of decade and season.

Figure 4.A1. Probability of warming, as a function of decade and season.
Figure 4.A2. Probability of precipitation increase, as a function of decade and season.

Figure 5.A1. Selected quantiles of the probability distribution of annual mean temperature change as a function of decade.
Figure 5.A2. As Figure 5.A1, but for winter mean temperature change.
Figure 5.A3. As Figure 5.A1, but for spring mean temperature change.
Figure 5.A4. As Figure 5.A1, but for summer mean temperature change.
Figure 5.A5. As Figure 5.A1, but for autumn mean temperature change.
Figure 5.A6. Selected quantiles of the probability distribution of annual mean precipitation change as a function of decade.
Figure 5.A7. As Figure 5.A6, but for winter mean precipitation change.
Figure 5.A8. As Figure 5.A6, but for spring mean precipitation change.
Figure 5.A9. As Figure 5.A6, but for summer mean precipitation change.
Figure 5.A10. As Figure 5.A6, but for autumn mean precipitation change.
Figure 5.A11. Probabilistic forecasts of temperature change at three grid boxes (Iceland, western Norway and Northern Finland), as function of decade and season.
Figure 5.A12. Probabilistic forecasts of precipitation change at three grid boxes (Iceland, western Norway and Northern Finland), as function of decade and season.

Figure 7.A1. Probability distributions of seasonal and annual mean temperature change at three grid boxes (Iceland, western Norway and Northern Finland): comparison between the resampling ensemble method and the normal distribution method.
Figure 7.A2. As Figure 7.A1, but for precipitation changes.

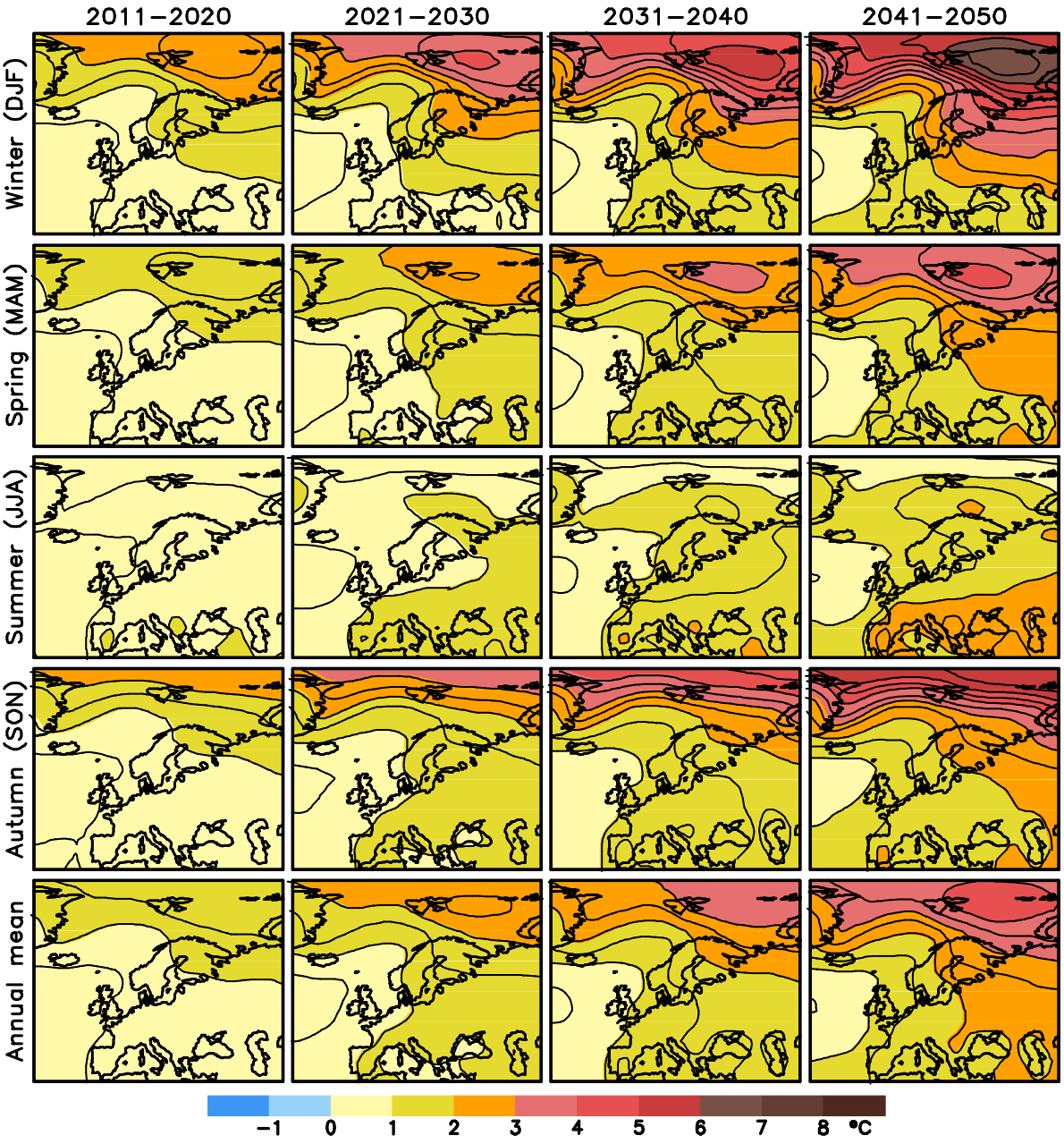

Figure 3.A1. *Best (median) estimates of temperature change from the period 1971-2000 to the periods indicated on the top of the figure, under the A1B emission scenario. Results are shown for four three-month seasons (winter = December-January-February; spring = March-April-May; summer = June-July-August; autumn = September-October-November) and for the annual mean. Shading interval is 1ºC, as indicated by the colour bar, and contours are drawn at every 0.5ºC.*

Figure 3.A2. *Best (median) estimates of precipitation change from the period 1971-2000 to the periods indicated on the top of the figure, under the A1B emission scenario. Results are shown for four three-month seasons (winter = December-January-February; spring = March-April-May; summer = June-July-August; autumn = September-October-November) and for the annual mean. Shading interval is 5%, as indicated by the colour bar.*

Figure 4.A1. *Probability of warming relative to the baseline period 1971-2000 under the A1B emission scenario. The periods and seasons are indicated on the horizontal and the vertical axis, respectively. For example, the map in the upper left corner gives the estimated probability that the winter (December-January-February) mean temperature, as averaged over the decade 2011-2020, will exceed the corresponding mean for 1971-2000. The colour scale is given below the figure.*

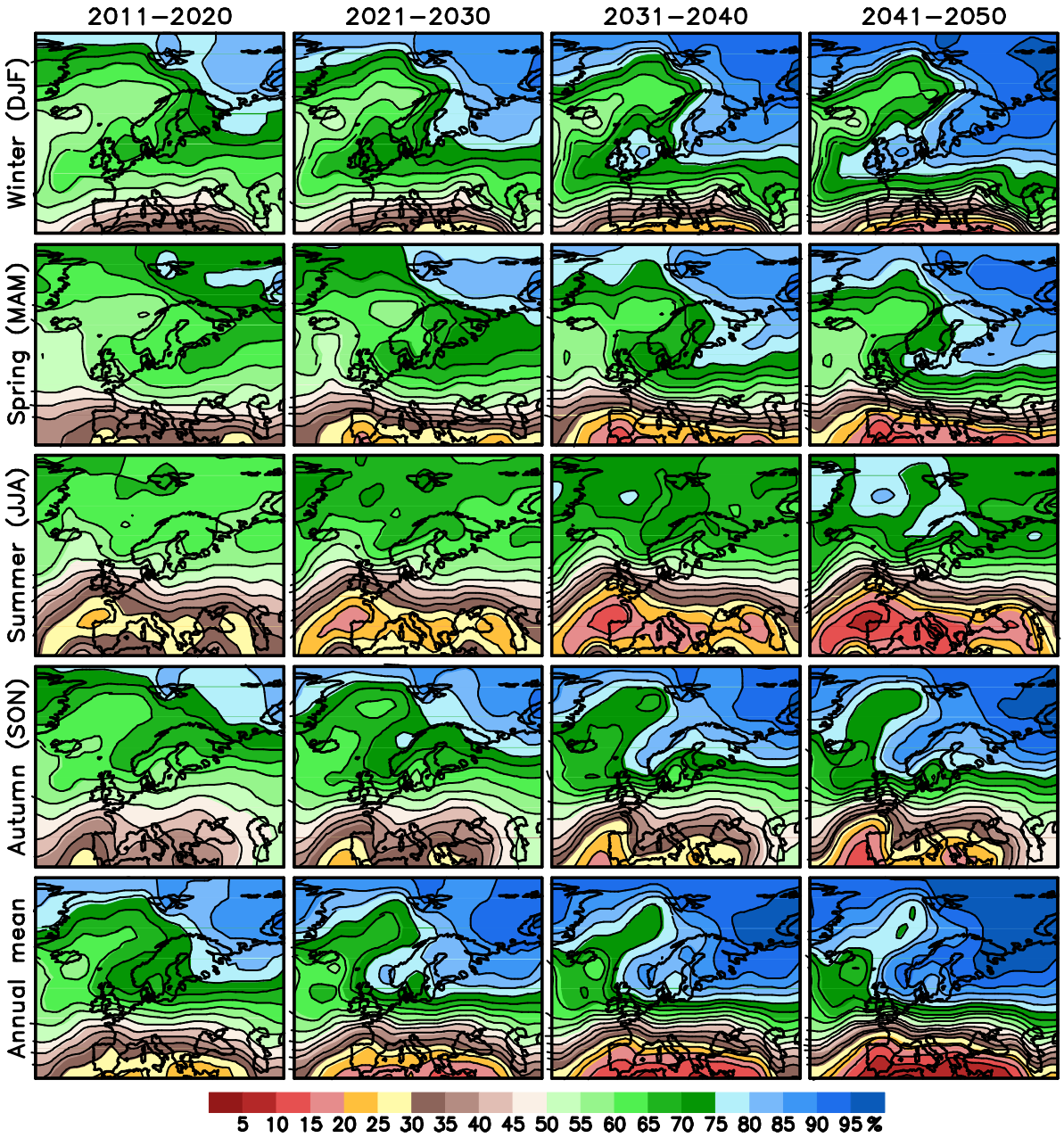

Figure 4.A2. *Probability that precipitation will exceed the mean value in 1971-2000 under the A1B emission scenario. The periods and seasons are indicated on the horizontal and the vertical axis, respectively. The colour scale is given below the figure.*

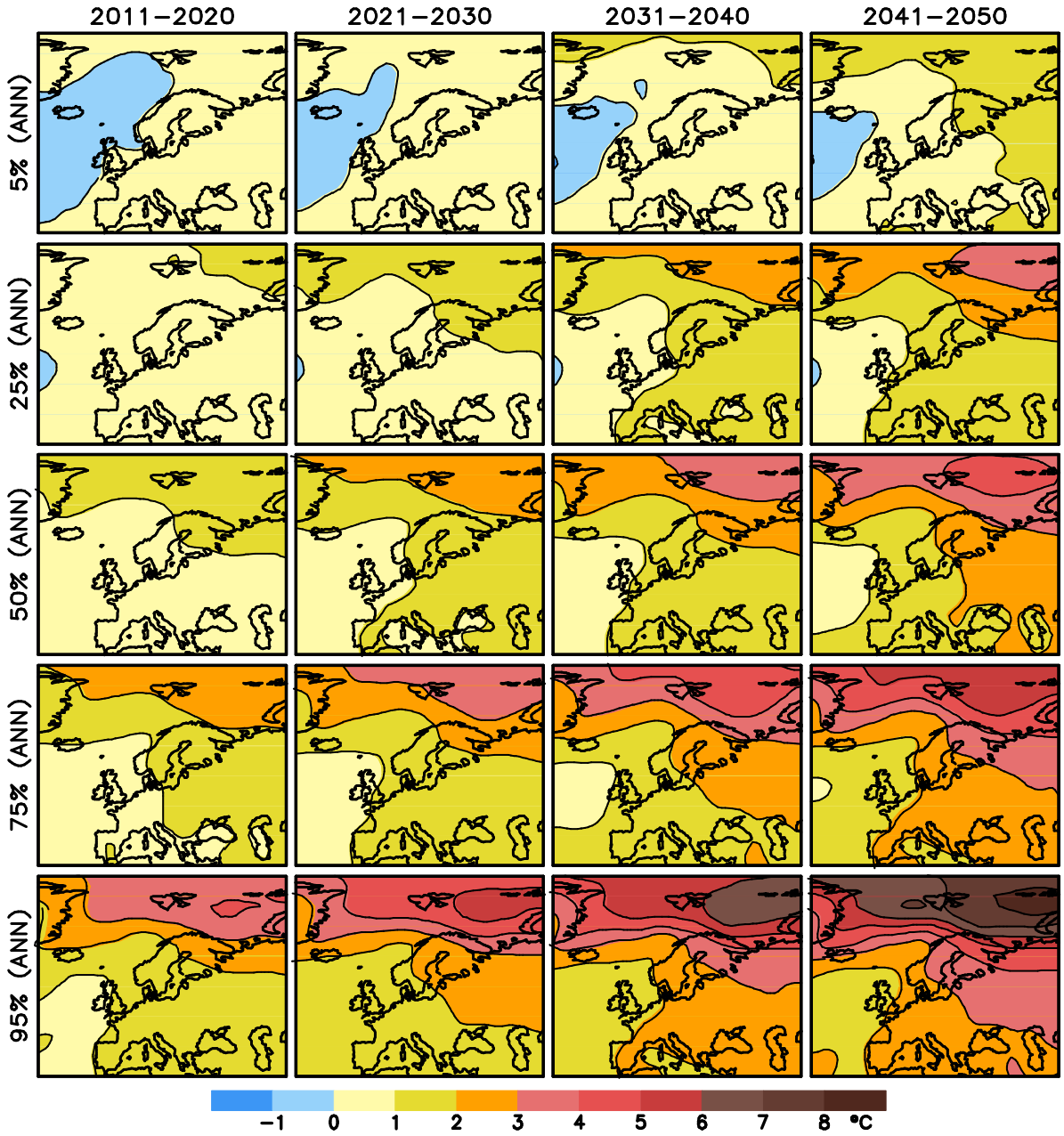

Figure 5.A1. *Quantiles of the probability distribution of annual mean temperature change relative to the baseline period 1971-2000, for the A1B scenario and for the periods indicated on the horizontal axis. There is, on the basis of the present model simulations, a 90% probability that the temperature changes in the real world will fall between the 5% and 95% quantiles, and a 50% probability for the interval between the 25% and 75% quantiles. The colour scale is given below the figure.*

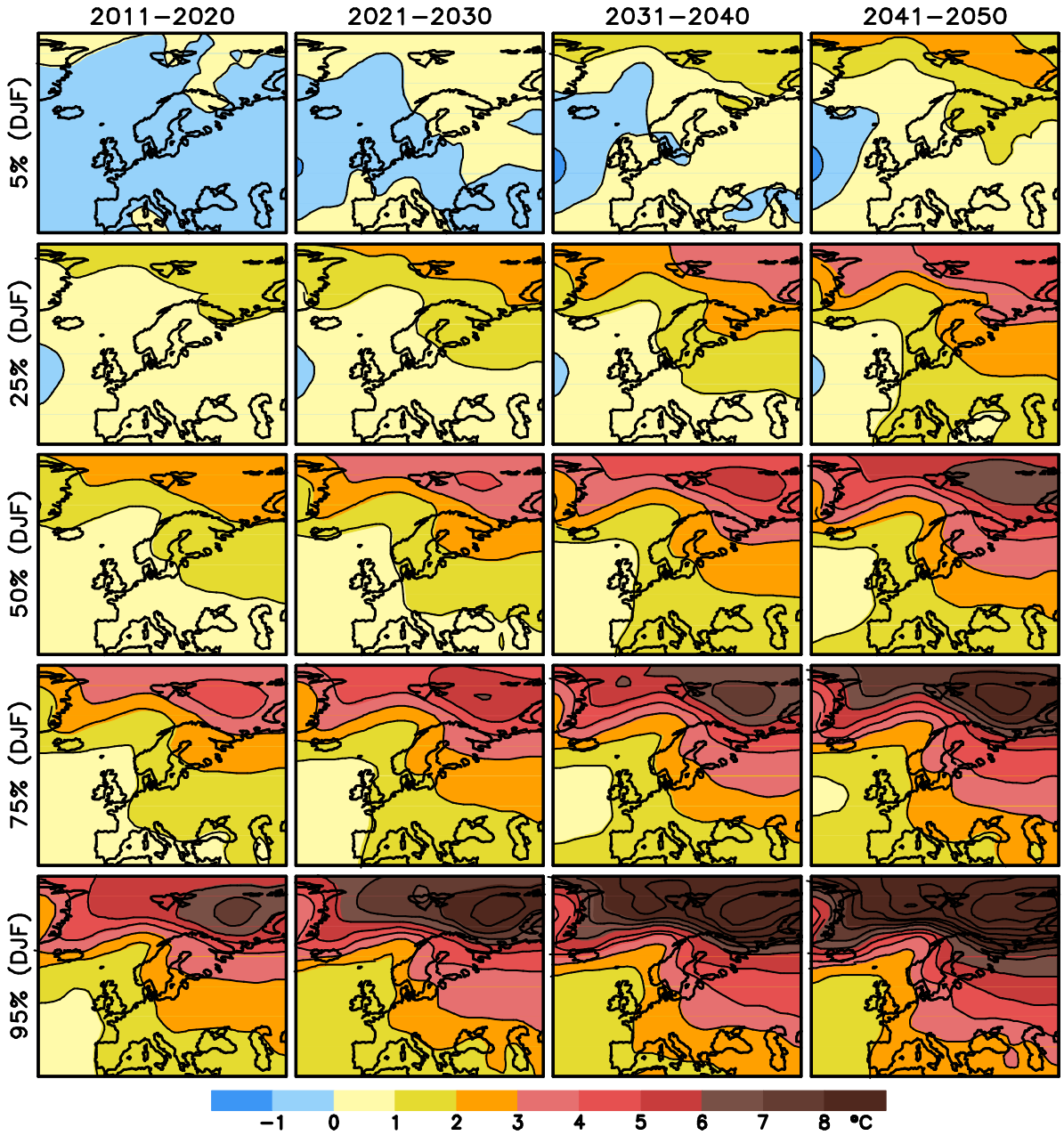

Figure 5.A2. *As Figure 5.A1, but for winter (December-January-February).*

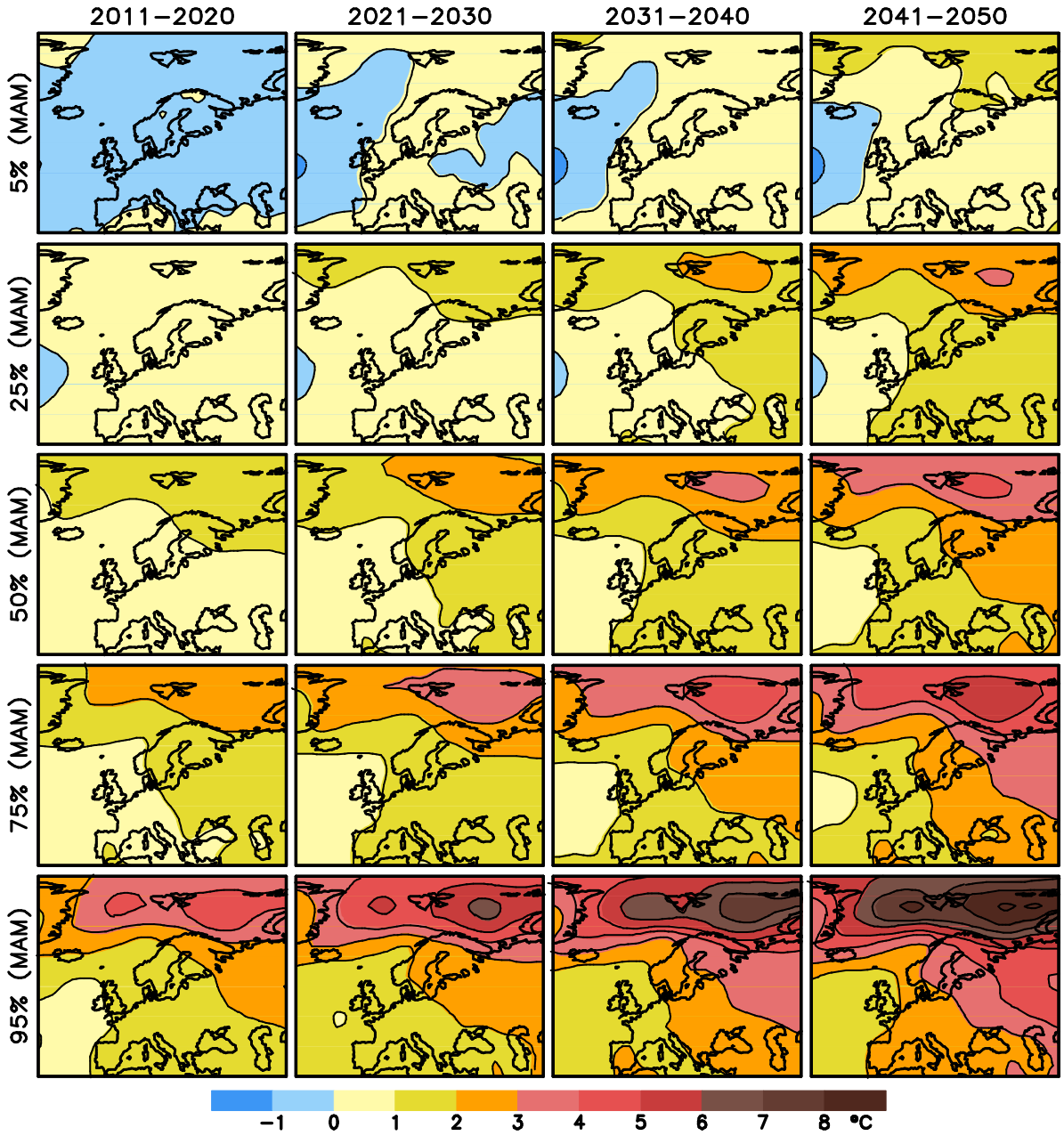

Figure 5.A3. *As Figure 5.A1, but for spring (March-April-May).*

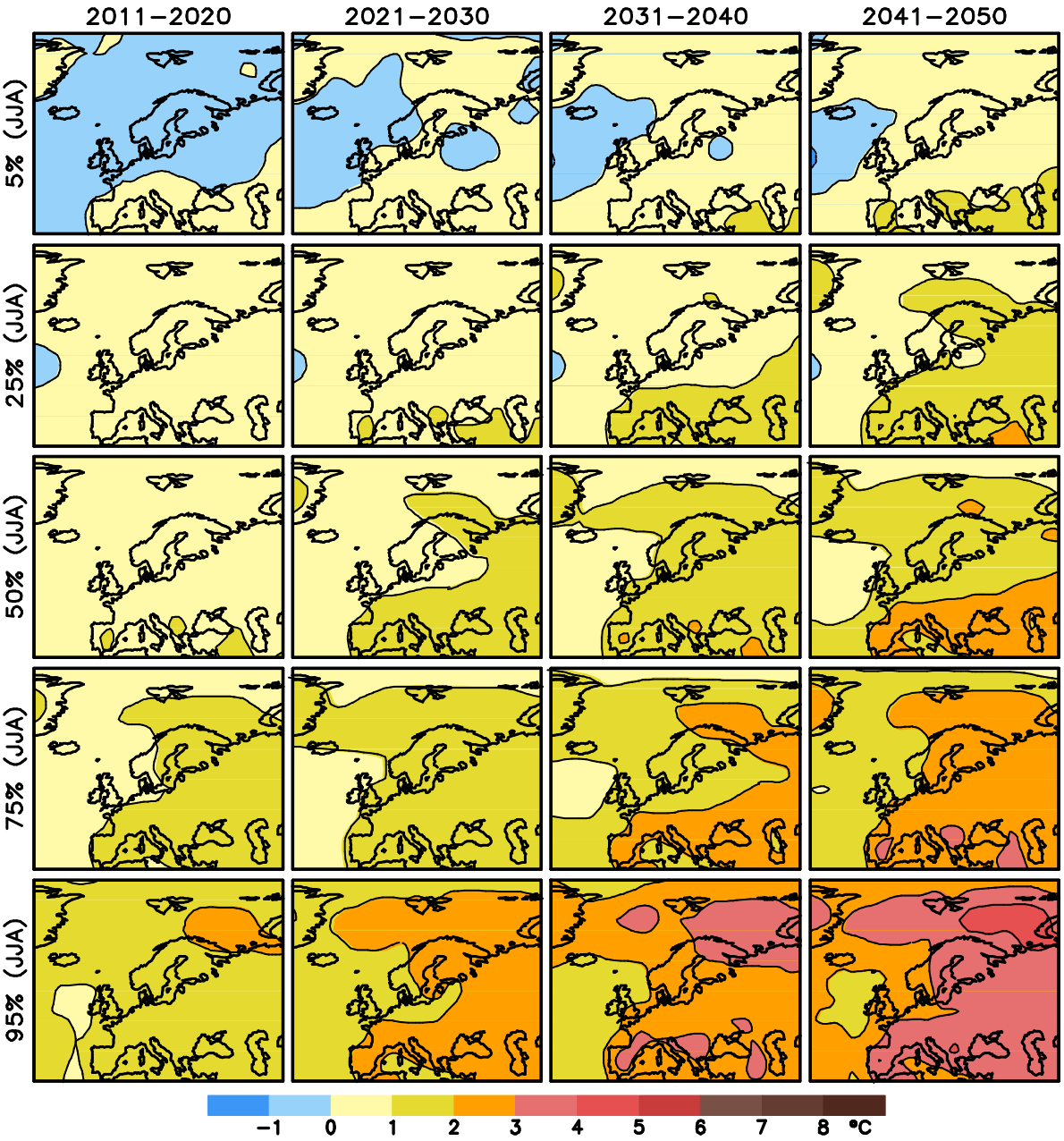

Figure 5.A4. *As Figure 5.A1, but for summer (June-July-August).*

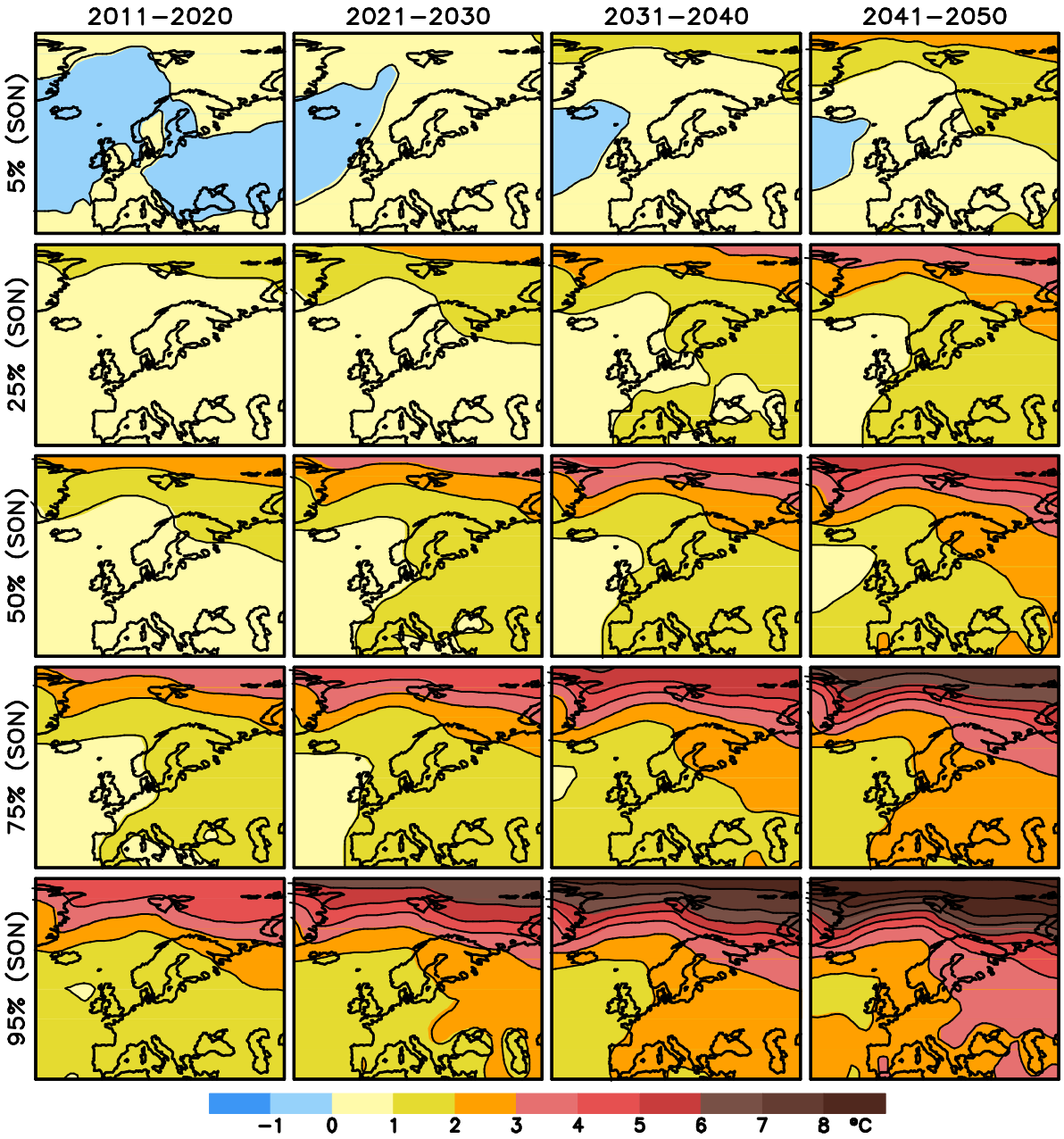

Figure 5.A5. *As Figure 5.A1, but for autumn (September-October-November).*

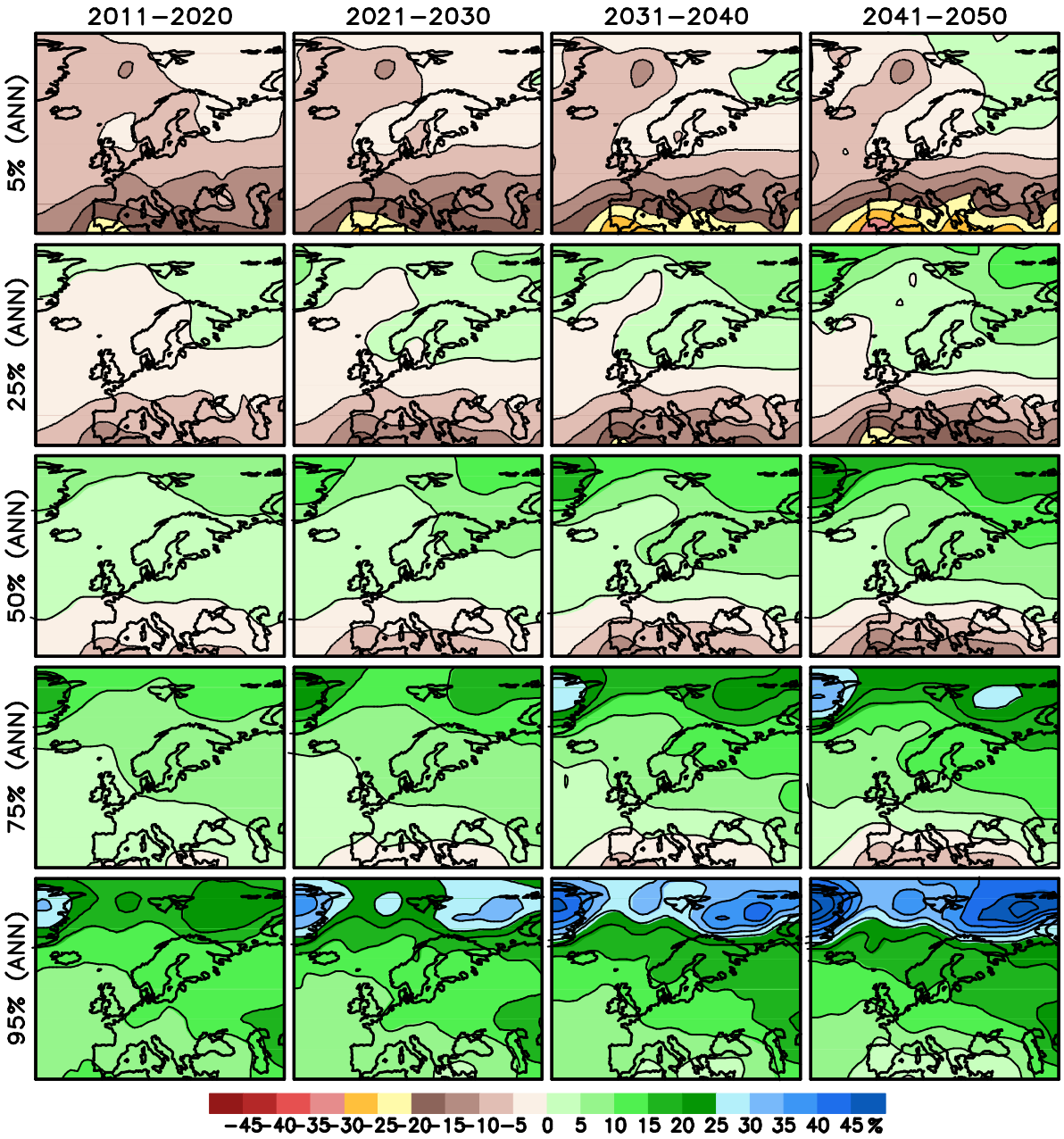

Figure 5.A6. *Quantiles of the probability distribution of annual mean precipitation change relative to the baseline period 1971-2000, for the A1B scenario and for the periods indicated on the horizontal axis. There is, on the basis of the present model simulations, a 90% probability that the precipitation changes in the real world will fall between the 5% and 95% quantiles, and a 50% probability for the interval between the 25% and 75% quantiles. The colour scale is given below the figure.*

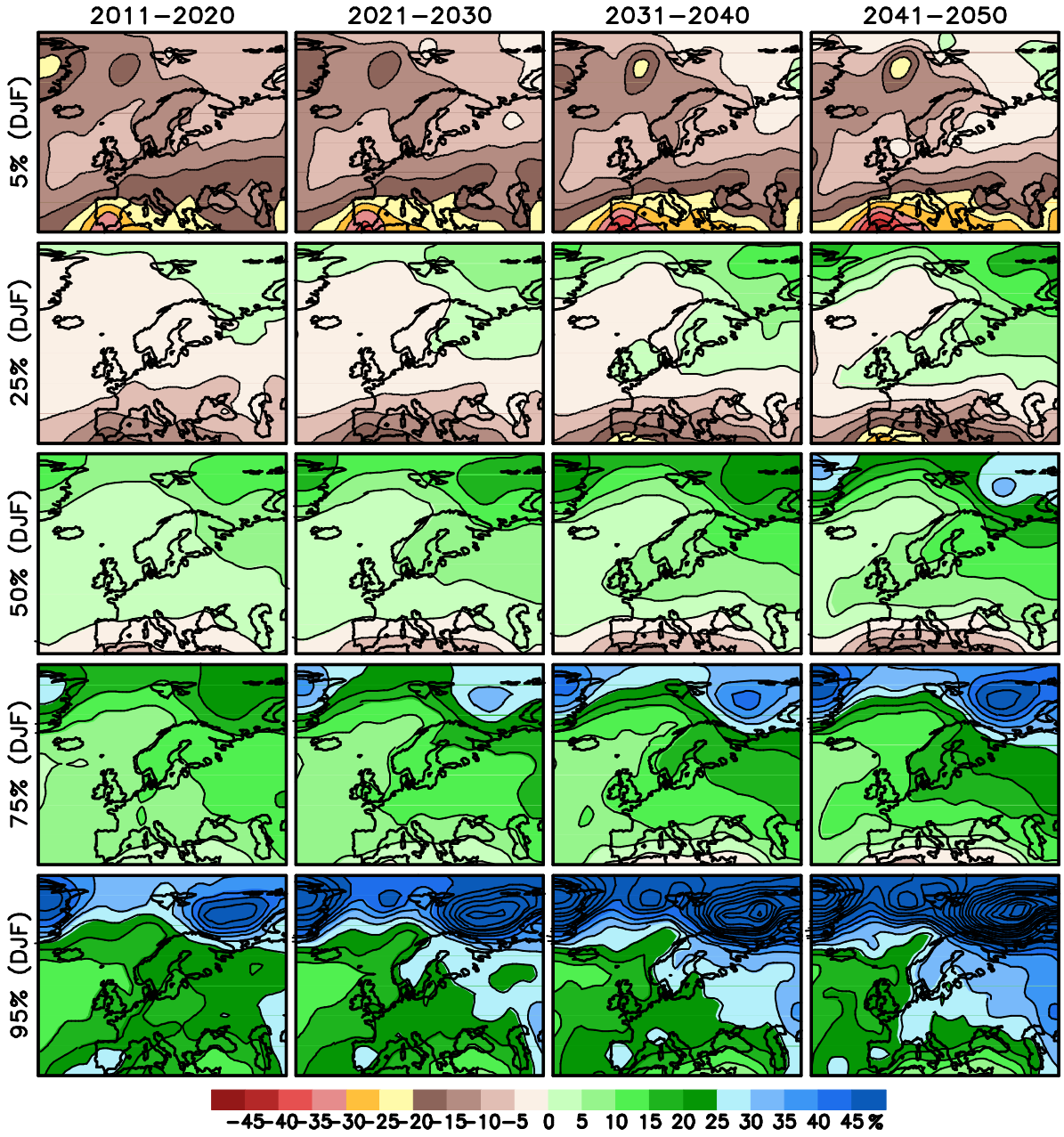

Figure 5.A7. *As Figure 5.A6, but for winter (December-January-February).*

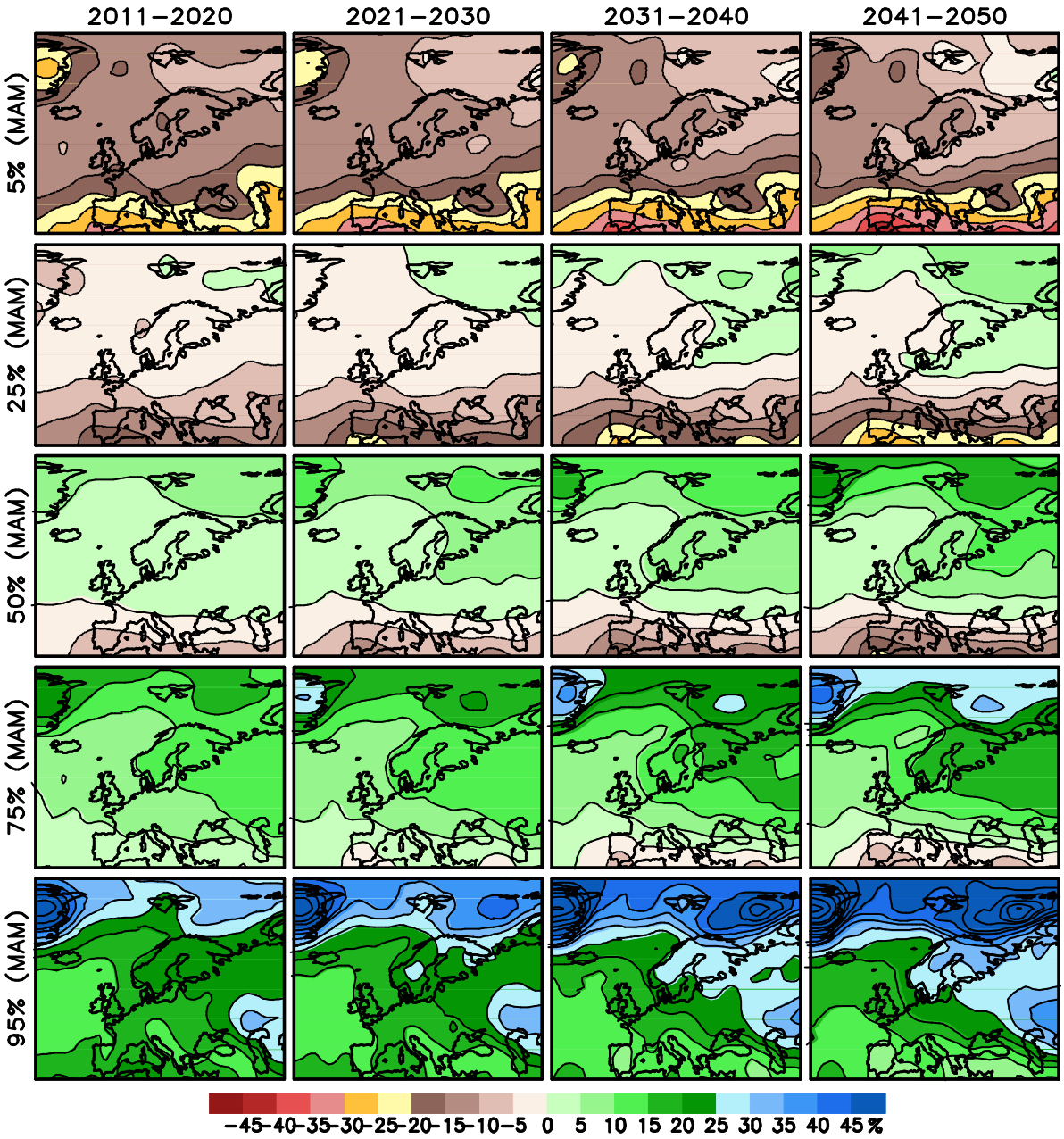

Figure 5.A8. *As Figure 5.A6, but for spring (March-April-May).*

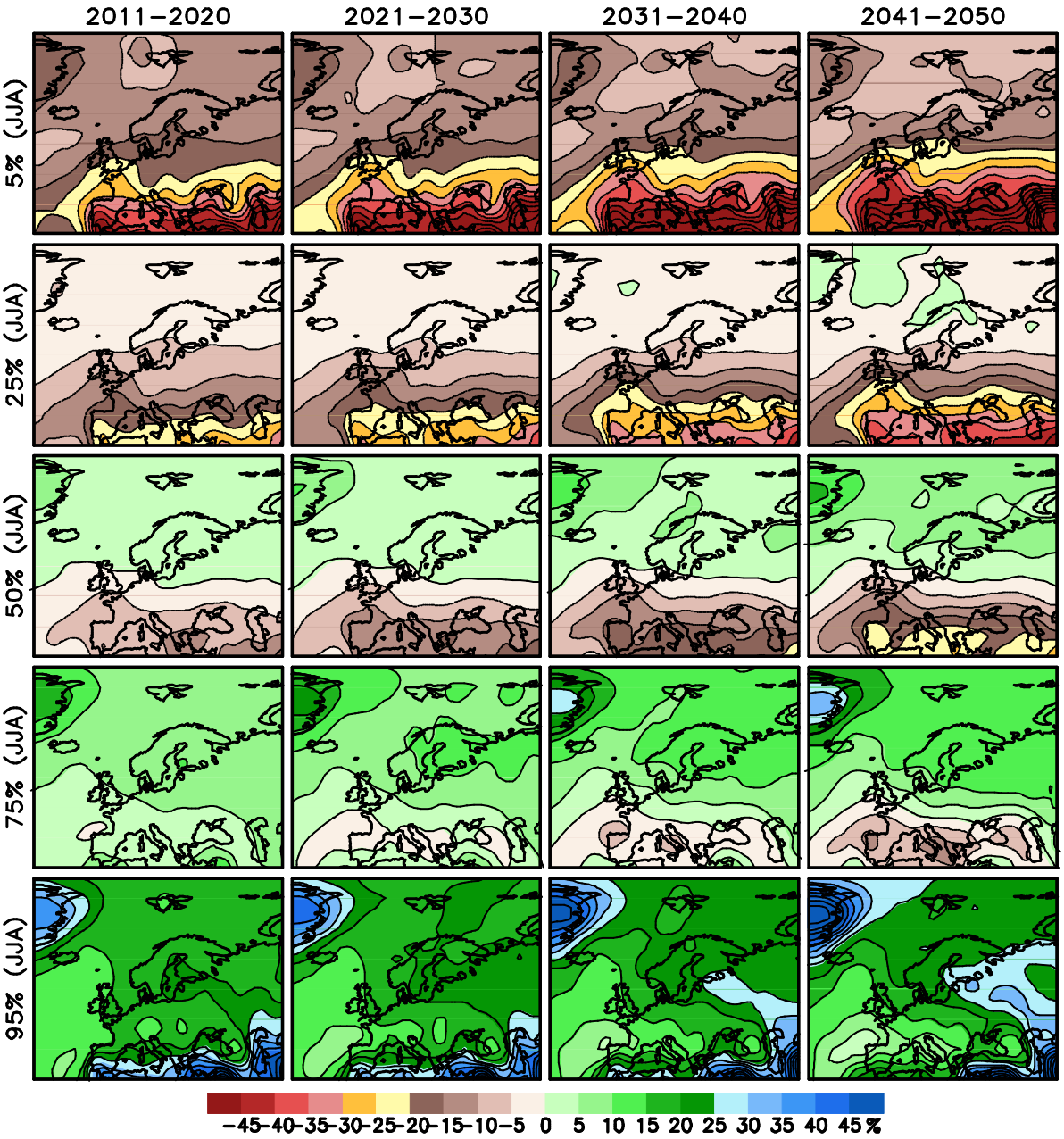

Figure 5.A9. *As Figure 5.A6, but for summer (June-July-August).*

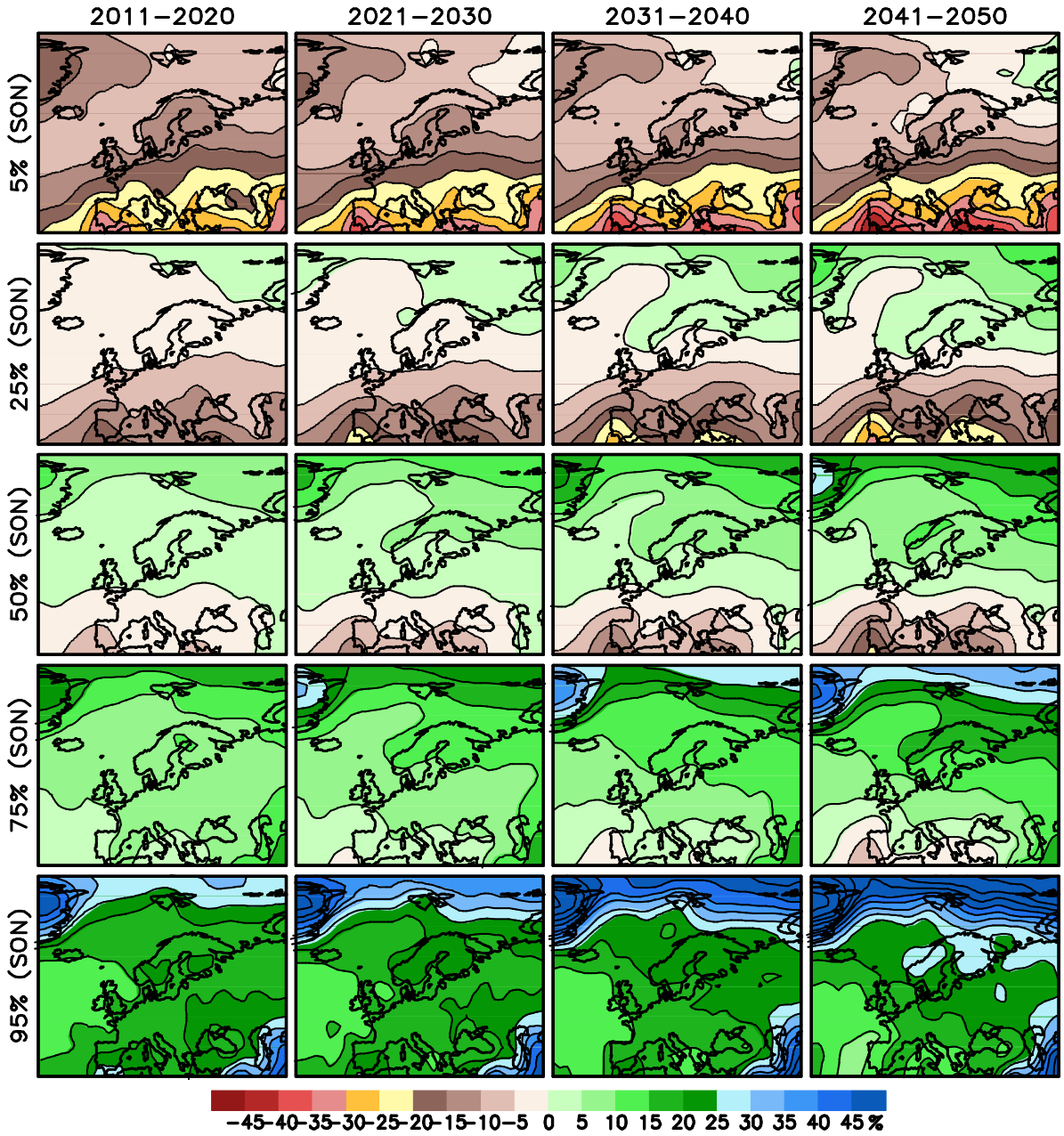

Figure 5.A10. *As Figure 5.A6, but for autumn (September-October-November).*

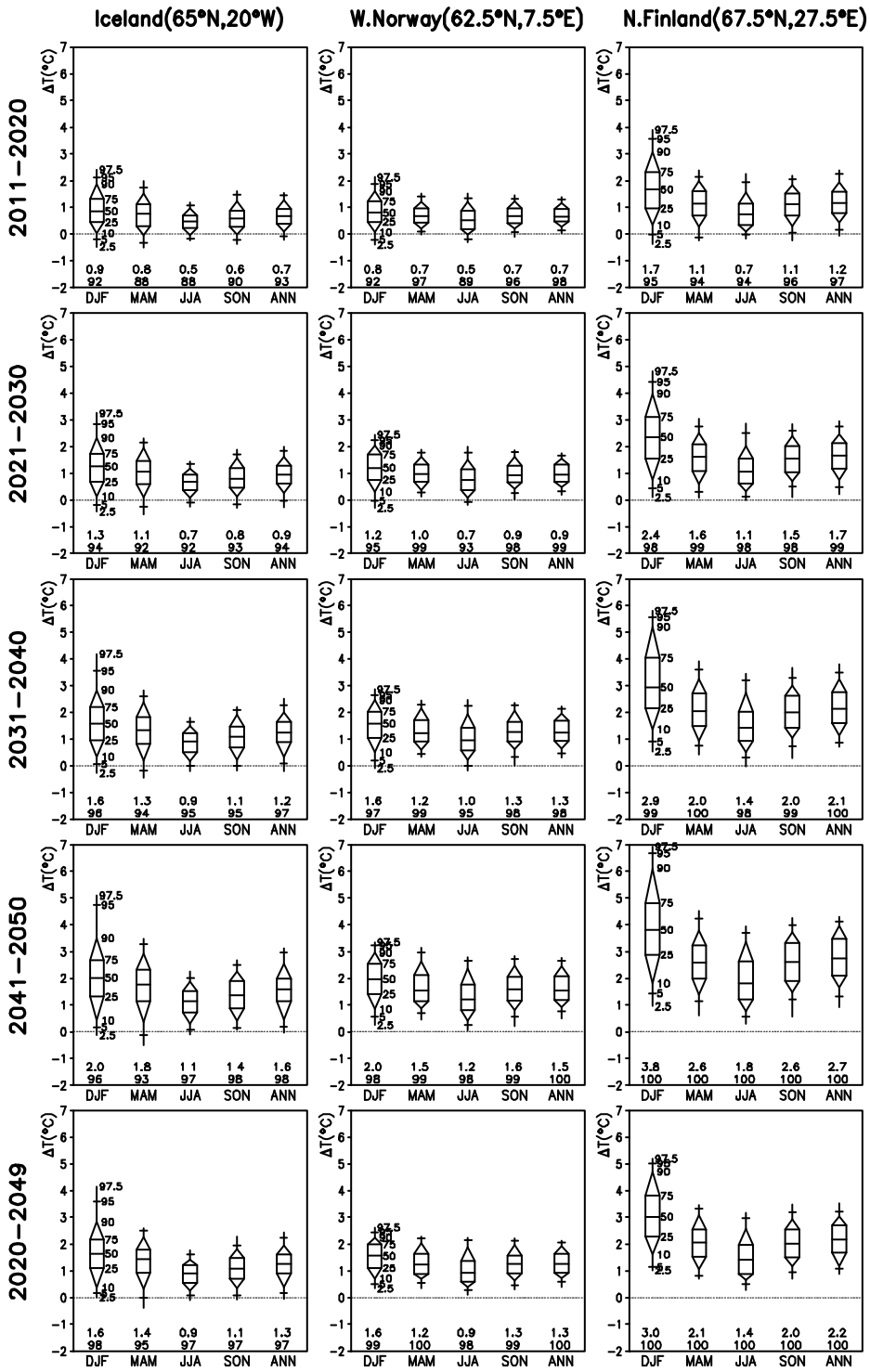

Figure 5.A11. *Probabilistic forecasts of temperature change for the three locations indicated on the top of the figure, for the A1B emission scenario and the periods indicated on the left. The diagrams show the 2.5%, 5%, 10%, 25%, 50%, 75%, 90%, 95% and 97.5% quantiles of the forecast distributions, which are given separately for the four three-month seasons and for the annual mean. The two numbers on the bottom give the median estimate of the change relative to the baseline 1971-2000 (in ºC), and the probability (in per cent) that the forecast period will be warmer than 1971-2000.*

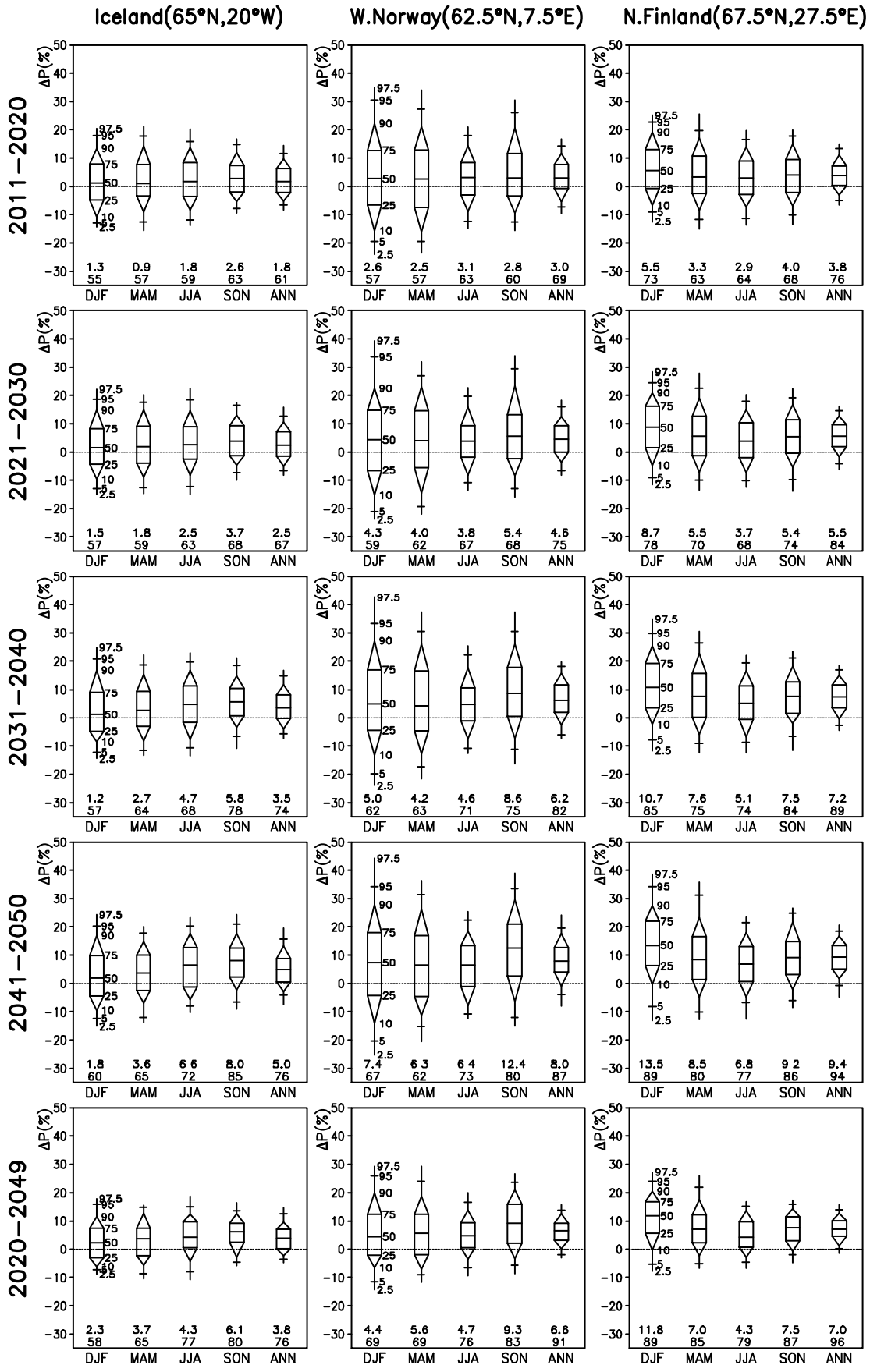

Figure 5.A12. *As Figure 5.A11, but for changes in precipitation expressed in per cent of the mean value for 1971-2000.*

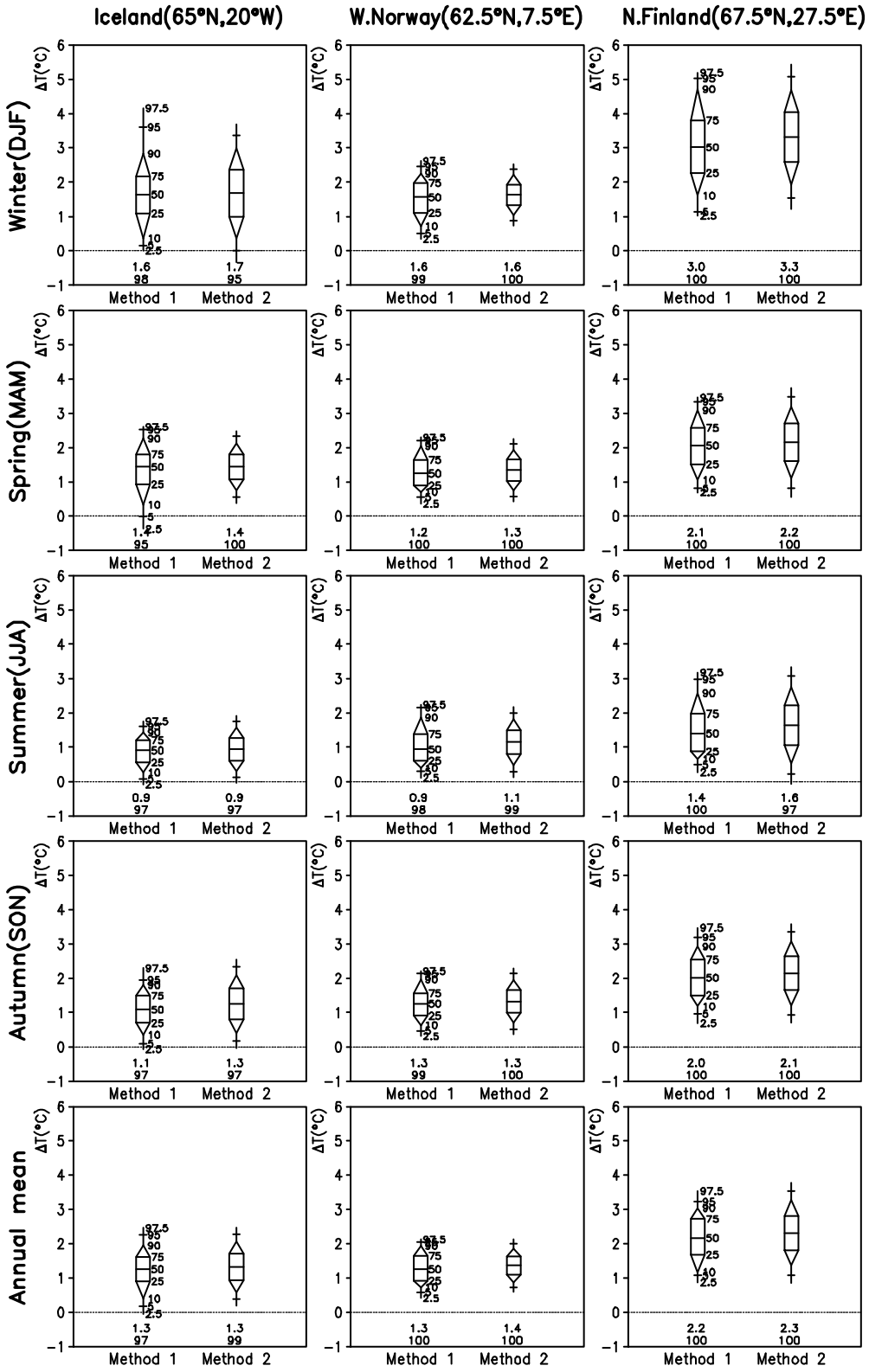

Figure 7.A1. *Probability distributions of seasonal and annual mean temperature change, from 1971-2000 to 2020-2049 under the SRES A1B scenario, at the three locations indicated on the top of the figure. Method 1 = resampling ensemble method; Method 2 = normal distribution method. The percentiles of the probability distributions are indicated in the same way as in Figure 5.3.*

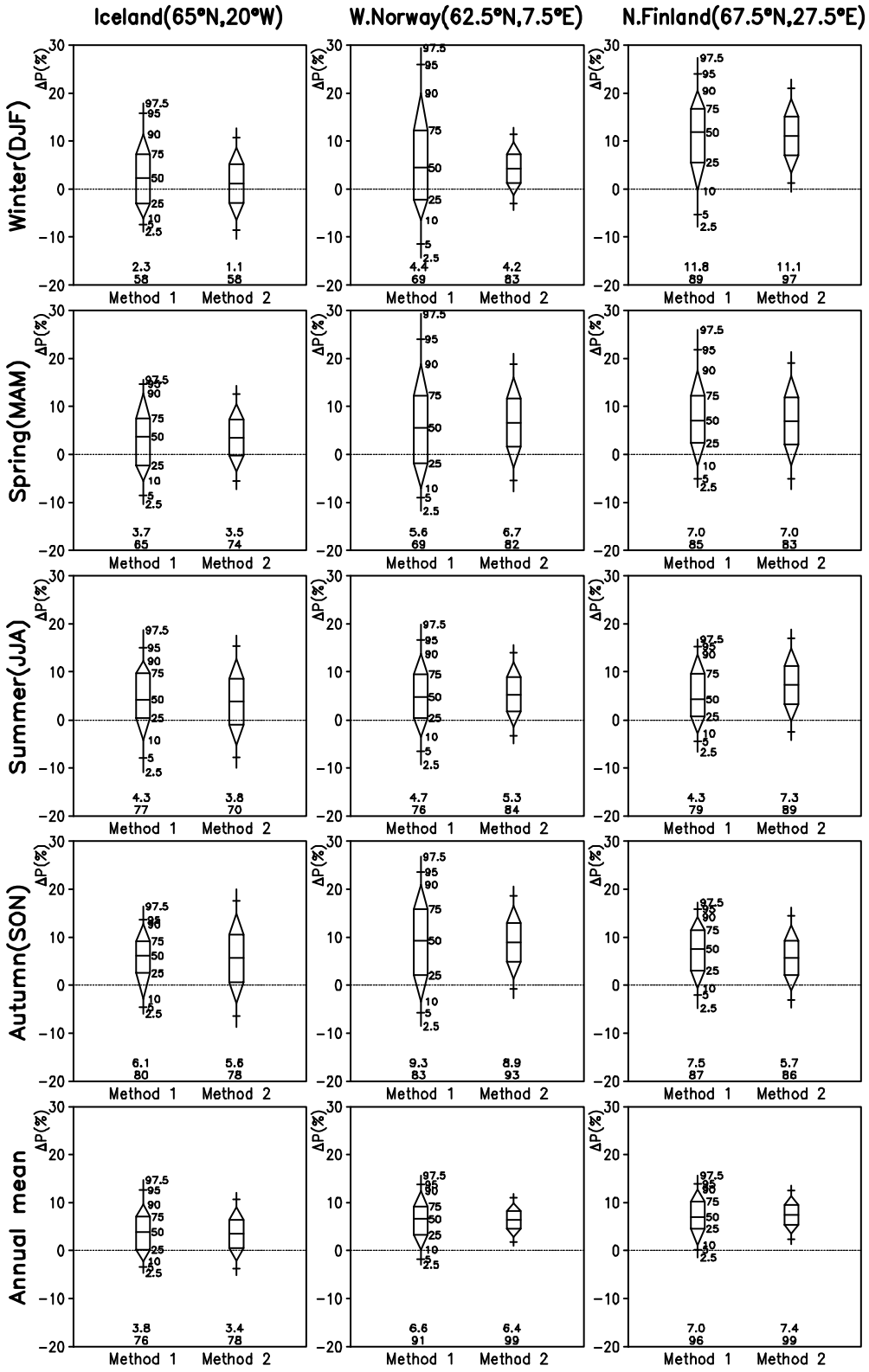

Figure 7.A2. *Probability distributions of seasonal and annual mean precipitation change, from 1971-2000 to 2020-2049 under the SRES A1B scenario, at the three locations indicated on the top of the figure. Method 1 = resampling ensemble method; Method 2 = normal distribution method. The percentiles of the probability distributions are indicated in the same way as in Figure 5.3.*